Since January 2020 Elsevier has created a COVID-19 resource centre with free information in English and Mandarin on the novel coronavirus COVID-19. The COVID-19 resource centre is hosted on Elsevier Connect, the company's public news and information website.

Brain, Behavior, and Immunity 112 (2023) 188–205

Contents lists available at ScienceDirect

Brain Behavior and Immunity

journal homepage: www.elsevier.com/locate/ybrbi

Fetal brain vulnerability to SARS-CoV-2 infection

Courtney L. McMahon [a,b], Joshua Castro [c], Jesus Silvas [c], Aranis Muniz Perez [a,b], Manuel Estrada [a,b], Ricardo Carrion Jr. [c], Jenny Hsieh [a,b,*]

[a] Department of Neuroscience, Developmental and Regenerative Biology, University of Texas at San Antonio, San Antonio, TX 78249, USA
[b] Brain Health Consortium, University of Texas at San Antonio, San Antonio, TX 78249, USA
[c] Texas Biomedical Research Institute, San Antonio, TX 78227, USA

ARTICLE INFO

Keywords:
COVID-19
SARS-CoV-2
Neurodevelopment
Neurotropism
Infection
Prenatal, gliosis, brain
Development

ABSTRACT

Whether or not SARS-CoV-2 can cross from mother to fetus during a prenatal infection has been controversial; however, recent evidence such as viral RNA detection in umbilical cord blood and amniotic fluid, as well as the discovery of additional entry receptors in fetal tissues suggests a potential for viral transmission to and infection of the fetus. Furthermore, neonates exposed to maternal COVID-19 during later development have displayed neurodevelopmental and motor skill deficiencies, suggesting the potential for consequential neurological infection or inflammation *in utero*. Thus, we investigated transmission potential of SARS-CoV-2 and the consequences of infection on the developing brain using human ACE2 knock-in mice. In this model, we found that viral transmission to the fetal tissues, including the brain, occurred at later developmental stages, and that infection primarily targeted male fetuses. In the brain, SARS-CoV-2 infection largely occurred within the vasculature, but also within other cells such as neurons, glia, and choroid plexus cells; however, viral replication and increased cell death were not observed in fetal tissues. Interestingly, early gross developmental differences were observed between infected and mock-infected offspring, and high levels of gliosis were seen in the infected brains 7 days post initial infection despite viral clearance at this time point. In the pregnant mice, we also observed more severe COVID-19 infections, with greater weight loss and viral dissemination to the brain, compared to non-pregnant mice. Surprisingly, we did not observe an increase in maternal inflammation or the antiviral IFN response in these infected mice, despite showing clinical signs of disease. Overall, these findings have concerning implications regarding neurodevelopment and pregnancy complications of the mother following prenatal COVID-19 exposure.

1. Introduction

Early into the pandemic, neurological symptoms began manifesting in COVID-19 patients, with over 30% of infected individuals having developed these complications, and up to 80% in those hospitalized (Mao et al. 2020; Poyiadji et al. 2020; Taherifard and Taherifard 2020; Helms et al. 2020). These complications range from mild to severe, with mild symptoms including but not limited to confusion, headache, anosmia, and ageusia, and more severe symptoms including seizure development, stroke, Guillain-Barre syndrome, and more (Mao et al. 2020; Arbour et al. 2000; Baig et al. 2020; Conde Cardona et al. 2020). In addition, more than 1/3 of patients have developed "long-COVID" accompanied by neurological complications such as brain fog, disorders with sleep, mood, or senses, myalgias, and sensorimotor deficits (Stefanou et al. 2022; Moghimi et al. 2021). These symptoms are suggestive of a viral neurotropism, but furthermore, SARS-CoV-2 has been detected in brain biopsies from fatal cases of COVID-19 with viral detection being seen in cortical neurons, glia, and choroid plexus cells (Crunfli et al. 2022; Song et al. 2021; Martin et al. 2022; Gomes et al. 2021; Reagan-Steiner et al. 2022). It has also been shown that many previous coronaviruses easily invade cells of the CNS (Arbour et al. 2000; Helms et al. 2020; Taherifard and Taherifard 2020; Poyiadji et al. 2020).

Abbreviations: COVID-19, coronavirus disease of 2019; SARS-CoV-2, severe acute respiratory syndrome coronavirus 2; ACE-2, angiotensin-converting enzyme 2; IFN, interferon; ABSL-3, Animal Biological Safety Level 3; MAP2, microtubule associated protein 2; TUJ1, beta-III Tubulin; 5HT2C, 5-hydroxytryptamin 2C; ChP, choroid plexus cells; ALDH1L1, aldehyde dehydrogenase 1 family member L1; SOX9, SRY-Box Transcription Factor 9; HSV, herpes simplex virus; HIV, human immunodeficiency virus; ESC, embryonic stem cell; FFU, focus-forming units; hpi, hours post infection; dpi, days post infection; TMPRSS2, transmembrane protease serine 2; CD31, cluster of differentiation 31; IHC, immunohistochemistry; IFC, imaging flow cytometry.

* Corresponding author at: One UTSA Circle, San Antonio, TX 78249, USA.

https://doi.org/10.1016/j.bbi.2023.06.015
Received 15 December 2022; Received in revised form 8 June 2023; Accepted 10 June 2023
Available online 16 June 2023

As the pandemic progressed, exposure to COVID-19 infection has increased exponentially. One of the more highly susceptible groups is that of pregnant women, with evidence showing a higher risk for severe infection development, as well as increased rates of pregnancy complications following a maternal case of COVID-19 (Jamieson and Rasmussen 2022; Zambrano et al. 2020; Reagan-Steiner et al. 2022). These reports have shown increased rates of preeclampsia, pre-term birth, miscarriages, and neurological complications such as developmental and motor skill deficits in neonates following maternal infection. A very recent study reported on severe neurological complications such as seizures, acquired microcephaly, and developmental delay after being exposed to maternal COVID-19 infections *in utero* (Benny et al. 2023). Additionally, SARS-CoV-2 has been detected in amniotic fluid and umbilical cord blood, with recent studies suggesting a potential for SARS-CoV-2 to infect the placenta and various tissues of the fetus (Baig et al. 2020; Aldrete-Cortez et al. 2022; Archuleta et al. 2022; Mesci et al. 2020; Varma et al. 2020; Reagan-Steiner et al. 2022). Importantly, many of these receptors are expressed in the fetal brain, and viral infection during pregnancy has long been associated with neuropsychiatric disorder development later in life, such as autism spectrum disorder, schizophrenia, bipolar disorder, and anxiety disorders (Al-Haddad et al. 2019; Baron-Cohen et al. 1999; Barry and Bary 1961; Burd, Balakrishnan, and Kannan 2012; Van Campen et al. 2020). Although direct infection of the viral pathogen may lead to the development of such disorders following prenatal exposure, maternal inflammation during pregnancy as a result of viral infection may also have detrimental consequences on neurodevelopment (Carlezon et al. 2019; Flaherman et al. 2020; Hava et al. 2006; Shi et al. 2003). With the higher risk of prenatal infection, the potential for SARS-CoV-2 to invade human brain tissue, and the implications of a COVID-19 infection and the resulting inflammation still poorly understood, a better understanding of the consequences of prenatal COVID-19 exposure on neurodevelopment is imperative.

Our previous studies on SARS-CoV-2 infection of the brain using *in vitro* models failed to fully replicate the intact system (McMahon et al. 2021). Thus, in an attempt to reveal some insight into this important topic, such as vertical transmission potential and offspring pathology, we used humanized mice which expressed human ACE2 in place of the endogenously expressed mouse ACE2 to replicate the effects of prenatal COVID-19 infection on the developing fetal brain. Here, we showed that viral transmission to the fetus was not only possible, but occurred at significant levels at later stages in development. We also demonstrated a tropism for various cells of the brain, such as neurons, glial cells, and barrier cells such as those of the choroid plexus, as well as endothelial cells of the blood vessels. Although we did not see increased cell death in the brain tissue, we did find concerning levels of gliosis in the pups 7 dpi and early gross developmental differences. These findings highlight the importance of preventative measures against COVID-19 during pregnancy.

2. Methods

2.1. Mouse strains and breeding

8-week old specific-pathogen-free male and female B6.129S2(Cg)-Ace2 < tm1(ACE2)Dwnt>/J (stock no. 035000) hACE2-KI (Zhou et al. 2021) and C57BL/6J (stock no. 000664) mice were purchased from The Jackson Laboratory (Bar Harbor, ME) and crossed to produce heterozygous hACE2-KI females, and hemizygous hACE2-KI and homozygous-wild type males. All experimental procedures were conducted following the National Institute of Health guidelines and were approved by the Institutional Animal Care and Use Committee (IACUC) at the University of Texas at San Antonio.

2.2. Mouse infections and sample processing

For the morbidity and mortality study and to determine viral titer, a total of 9 hACE2-KI female heterozygous mice were randomly assigned to one of 4 treatment groups (3 mice per group): mock infection or one of three viral titers. The female mice were bred with hemizygous hACE2-KI males or wild type C57BL/6J males overnight to produce litters with mixed genotypes, then transferred to the ABSL3 and housed in microisolator cages with sterile water and chow *ad libitum*. Mice were infected intranasally (i.n.) with either mock (PBS) or with 10, 10^3, or 10^5 FFU of delta variant SARS-CoV-2, isolate hCoV-19/USA/PHC658/2021 (Lineage B.1.617.2) in a final volume of 60 μl following isoflurane sedation. After viral infection, mice were monitored daily for 4 dpi for morbidity (body weight loss) and mortality (survival). No mice lost more than 20% of their initial body weight, but were euthanized at 4 dpi. Lung, spleen, and brain tissues were harvested and homogenized in 2 mL of PBS. Tissue homogenates were centrifuged at 3,900 rpm for 15 min and supernatants were collected for genomic RNA and subgenomic mRNA RT-qPCR analysis.

For prenatal infection studies, 8–12-week old heterozygous hACE2-KI females were bred with hemizygous hACE2-KI males or wild type C57BL/6J males overnight to produce litters with mixed genotypes. Pregnant mice were then transferred to the ABSL3 at E12 or E16.5 and housed in microisolator cages with sterile water and chow *ad libitum*. Mice were randomly assigned to treatment groups and immediately infected intranasally (i.n.) at either E12.5 or E16.5 with mock (PBS) or with 10^5 FFU of delta variant SARS-CoV-2, isolate hCoV-19/USA/PHC658/2021 (Lineage B.1.617.2) in a final volume of 60 μl following isoflurane sedation. After viral infection, mice were monitored daily for morbidity (body weight loss) and euthanized at 48 hpi based on the previous morbidity and viral titer study. In some experiments, pregnant mice were infected at E16.5 with mock (PBS) or 10^5 FFU of delta variant SARS-CoV-2 and the pups were euthanized at 7 dpi. Mice were perfused with PBS, then the lung, spleen, and brain tissues were harvested from the dam. The uterus was also harvested to collect the placentas, fetal brains, thoracic, cardiac, and abdominal tissues. For RT-qPCR analyses, all tissues were homogenized in 2 mL of PBS, then tissue homogenates were centrifuged at 3,900 rpm for 15 min and supernatants were collected for genomic RNA and subgenomic mRNA RT-qPCR analysis. Fetal tails were collected for genotyping and sexing. For other analyses, pregnant dams were anesthetized using isoflurane, then cheek blood was collected for serum harvesting. The dams were then perfused using sterile PBS and 4% PFA. Following PBS perfusion, the lungs were collected from the dams and homogenized in TRIzol for RT-qPCR to confirm infection. Following PFA perfusion, the brain of the dam, the placentas, and the fetuses were collected and placed in 10% neutral buffered formalin for 72 h in order to conduct IHC.

2.3. RNA isolation

Virus-infected tissues were inactivated by mixing homogenized samples with TRIzol Reagent (Life Technologies) in clean screw-top micro-centrifuge tubes. Viral RNAs were extracted from the inactivated samples using an EpMotion M5073c Liquid Handler (Eppendorf) and the NucleoMag Pathogen kit (Macherey-Nagel). Briefly, 10μg yeast tRNA and 1×10^3 pfu of MS2 phage were added to each sample. After centrifugation, the aqueous phase was transferred to a new tube containing NucleoMag B-Beads and binding buffer, and the samples were mixed for 10 min at room temperature. RNA extraction was completed on the liquid handler according to the NucleoMag Pathogen kit protocol. The isolated RNAs were quantified using a NanoDrop One spectrophotometer (Thermo Fischer Scientific).

2.4. Quantitative Real-Time PCR analysis for quantification of SARS-CoV-2 Genome Equivalents per mL

RT-qPCR was performed on a QuantStudio 3 instrument (Applied Biosystems) using the TaqPath™ 1-Step RT-qPCR Master Mix, CG (Thermo Fisher) and the following cycling parameters: Hold stage 2 min at 25 °C, 15 min at 50 °C, 2 min at 95 °C; PCR stage 45 cycles of 3 s at 95°Cm 30 s at 60 °C The CDC-developed 2019-nCoV_N1 assay was used to measure the quantity of Genome Equivalents (GE). Standard curve method was used for GE number calculations. The cut-off for positivity (limit of detection, LOD) was established at 10 GE per reaction (800 GE/mL). Samples were tested in duplicate.

2.5. Subgenomic qPCR analysis

RT-qPCR was also performed to measure subgenomic RNA of E region (Envelope). The assay was designed as described in Wolfel et al., 2020 (Wölfel et al. 2020). The same instrument, reaction master mix, and cycling parameters as for the genomic RNA quantification were used. LOD was set as 13.98 copies per reaction (800 copies/mL). Samples were tested in duplicate.

2.6. Imaging flow cytometry

Whole infected fetal brains were harvested and dissociated in a 10 mg/mL collagenase solution with 10% FBS for 1 hr. Cells were then stained with a viability dye (Zombie Aqua™, BioLegend, 423,101 or Zombie Yellow™, BioLegend, 423103) for 15 mins then fixed in 4% PFA for 1 hr. After incubation, cells were blocked and permeabilized using Ebioscience™ Intracellular Fixation & Permeabilization Buffer Set (Thermo, 88–8824-00) then incubated for 30 min at 4 °C with the following primary antibodies: human anti-SARS-CoV-2 spike protein conjugated with Alexa Fluor™ 647 (Thermo, 51–6490-82), rabbit anti-SOX9 (Thermo, MA5-41174), goat anti-hACE2 (R&D Systems, AF933), rabbit anti-beta-3 tubulin (Thermo, PA5-52655), chicken anti-MAP2 (Thermo Fisher, PA1-10005), rabbit anti-Nestin (Thermo Fisher, PA5-82905), rat anti-GFAP (Thermo Fisher, 13–0300), rabbit anti-Iba1 (Wako Chemicals, HNM3505),rabbit anti-Iba1 (Wako Chemicals, 019–19741), and rabbit anti-5HT2C (Abcam, ab133570). DAPI was added following secondary incubation at RT for 30 min in the dark with the following secondary antibodies at 1:1000: Alexa Fluor™ 488, and Cy3. Samples were then fixed for 72 hr with 4% PFA and analyzed with an ImageStreamX MKII (Millipore, Burlington, MA) image flow cytometer with a 7-μm core at low flow rate and high sensitivity using INSPIRE software. 50,000 single cells were randomly sampled from whole fetal brain dissociations. Fluorochromes were excited with 405, 488, 561, and 633 nm lasers and image data were collected through a 60 × objective in appropriate channels. Single-color reference samples for each fluorochrome were generated by inclusion of cells that are incubated with each fluorochrome separately. Images were analyzed using IDEAS® software version 6.2 (Millipore, Burlington, MA). A compensation matrix was built with the data from single-color reference samples to allow removal of spectral spillover to adjacent channels from each detection channel.

2.7. ELISA assays

Concentrations of cytokines from serum harvested from mock and infected dams were measured by ELISA using commercial kits specific for mouse cytokines (Signosis, EA-4003), mouse IFN-alpha/beta RD (Thermo, EM39RB), and mouse IFN gamma (Thermo, BMS606-2) according to the manufacturer's protocols. Briefly, samples were mixed with a diluent and were aliquoted in duplicate into microtiter strip wells coated with respective biotin-conjugated antibodies. Antibodies labeled with streptavidin-horseradish peroxidase were then added to the wells and incubated for 1 h at room temperature. After the incubation, wells were washed three times before addition of enzyme substrate. Samples were then incubated for 30 min. The resulting yellow acid dye at 450 nm with a reference filter of 620 nm was measured by a plate reader.

2.8. Immunofluorescence and confocal microscopy

Fetal mouse samples were fixed for 72 hr in 10% neutral buffered formalin, then transferred to 30% sucrose solution at 4 °C for 5 d. The tissues were then embedded in OCT Compound (Thermo Fischer Scientific) and sectioned at 20 μm on a standard cryostat using Fisherbrand™ Superfrost™ Plus Microscope Slides to collect sections. Sections were blocked and permeabilized for 1 hr at RT using 0.3% Triton and 1% donkey serum buffer, then incubated overnight at 4 °C with the following primary antibodies: human anti-SARS-CoV-2 spike protein conjugated with Alexa Fluor™ 647 (1:200, Thermo, 51–6490-82), human anti-igG1 isotype control conjugated with Alexa Fluor™ 647 (1:200, Novus Biologicals, DDXCH01A647-100), goat anti-CD31 (1:300, R&D Systems, AF3628), rabbit anti-ALDH1L1 (1:750, Abcam, ab177463), goat anti-hACE2 (1:50, R&D Systems, AF933), rabbit anti-beta-3 tubulin (1:50, Thermo, PA5-52655), chicken anti-MAP2 (1:2000, Thermo Fisher, PA1-10005), rabbit anti-Iba1 (1:1000, Wako Chemicals, HNM3505), and rabbit anti-5HT2C (1:500, Abcam, ab133570). DAPI was added following secondary incubation at RT for 30 min in the dark with the following secondary antibodies at 1:1000: Alexa Fluor™ 488, and Cy3. Slides were washed in TBS in between each incubation. Images from the cortical and hippocampal regions of the fetal brain were acquired using a Zeiss LSM 710 Confocal Microscope equipped with four laser lines (405, 488, 561, and 633 nm) under 20X and 40X objective lenses, and Zen 2011 software. Serial Z-stack images were collapsed to obtain a maximum intensity projection of lines after acquisition. Compared samples were processed in parallel, and the same settings and laser power were used for confocal microscopy.

2.9. Statistical analysis

SigmaPlot power analysis of previous work was used to determine sample size for each experiment (Lodge and Grace 2007; Elam et al. 2022). All data reported as mean ± standard error of the mean (SEM) unless otherwise indicated. Differences were considered statistically significant when $p < 0.05$ and are signified by $*p < 0.05$, $**p < 0.01$, $***p < 0.001$, and $****p < 0.0001$, and not statistically significant when p greater than 0.05, signified by n.s. In all cases, the stated n value represents individual mice. For IHC, compared samples were processed in parallel, and the same settings and laser power were used for confocal microscopy. Outliers were defined by performing Grubb's test. Student t-tests and repeated measures one-way ANOVA were used to evaluate statistical significance, using Bartlett's test to verify sphericity in multivariate analyses. All statistical analyses were conducted using GraphPad Prism software (version 9.3.1).

3. Results

3.1. Heterozygous hACE2 mice are susceptible to SARS-CoV-2 infection

Many previous studies of SARS-CoV-2 have utilized homozygous hACE2-KI mice, with few conducting infections in heterozygous mice (Winkler et al. 2022; Rathnasinghe et al. 2020; Zhou et al. 2021; Moreau et al. 2020; Zhang et al. 2022). In our studies, we aimed to evaluate the effects of fetal viral infection as well as maternal inflammation independent of fetal viral infection on the developing brain, thus we utilized heterozygous female hACE2-KI mice (Zhou et al. 2021) in order to generate litters containing both SARS-CoV-2-susceptible (hACE2+) and SARS-CoV-2-resistant (hACE2-) fetal genotypes. To validate our heterozygous hACE2-KI mice as a model for prenatal COVID-19 infection, we first conducted a titer-dependency assay to determine optimal viral titer for infection and a time line of peak viral infection. 12-week old

nonpregnant heterozygous hACE2-KI female mice were intranasally infected with PBS as a mock infection, or a maximum viral titer of 10^5 focus forming units (FFU) based on previous literature (Ye et al. 2021; An et al. 2021; Winkler et al. 2022). Two viral titers below this maximum titer (10 and 10^3 FFU) were additionally chosen to optimize infection while minimizing dose-related side effects. Weight and clinical signs of disease were monitored daily until mice reached 100% of their pre-infection body weight (4 dpi), and then the lungs, spleen, and brain were harvested for RT-qPCR analysis of viral load (Fig. S1A).

Mice in the mock infection and experimental groups 10 and 10^3 FFU did not display any weight loss or signs of disease, though mice in the 10^5 FFU group lost 20% of their pre-infection body weight within 48 hpi and displayed signs of disease including appetite loss, hunched posture, and ruffled fur. Interestingly, these mice displayed 100% body weight recovery at 72 hpi, which may be attributed to less hACE2 expression as a result of their heterozygous phenotype (Fig. S1B). RT-qPCR analysis of harvested tissues at 4 dpi showed infection in the lungs at 10^3 and 10^5 FFU, with a significant increase in viral load at 10^5 FFU. Infection was only observed in the spleen at 10^5 FFU, indicating that viral dissemination occurred at this viral titer, but no infection was observed in the brain (Fig. S1C). Subgenomic mRNA analysis showed that viral transcription (an indicator of viral replication) only occurred in the lungs of mice in the 10^5 FFU group (Fig. S1D). Comparable to infections seen in studies using homozygous hACE2-KI mice (Winkler et al. 2022; Rathnasinghe et al. 2020), these data validated our heterozygous hACE2-KI mice as a model for infection, and allowed us to identify 48 hpi as the peak infection time, and 10^5 FFU as optimal viral titer for subsequent experiments.

3.2. *Pregnant mice demonstrate more severe SARS-CoV-2 infection than nonpregnant mice, and viral infection was detected in the brains of pregnant mice*

For prenatal COVID-19 exposure studies, 8–12-week-old female heterozygous hACE2-KI mice were crossed to either hemizygous hACE-2 KI males or WT males in order to achieve desired fetal genotypes within each litter (Fig. S2). Desired fetal genotypes within each litter included both hACE2+ and hACE2- fetuses in order to evaluate the effects of fetal viral infection or maternal inflammation without fetal viral infection, respectively. Timed pregnancies were used to determine the

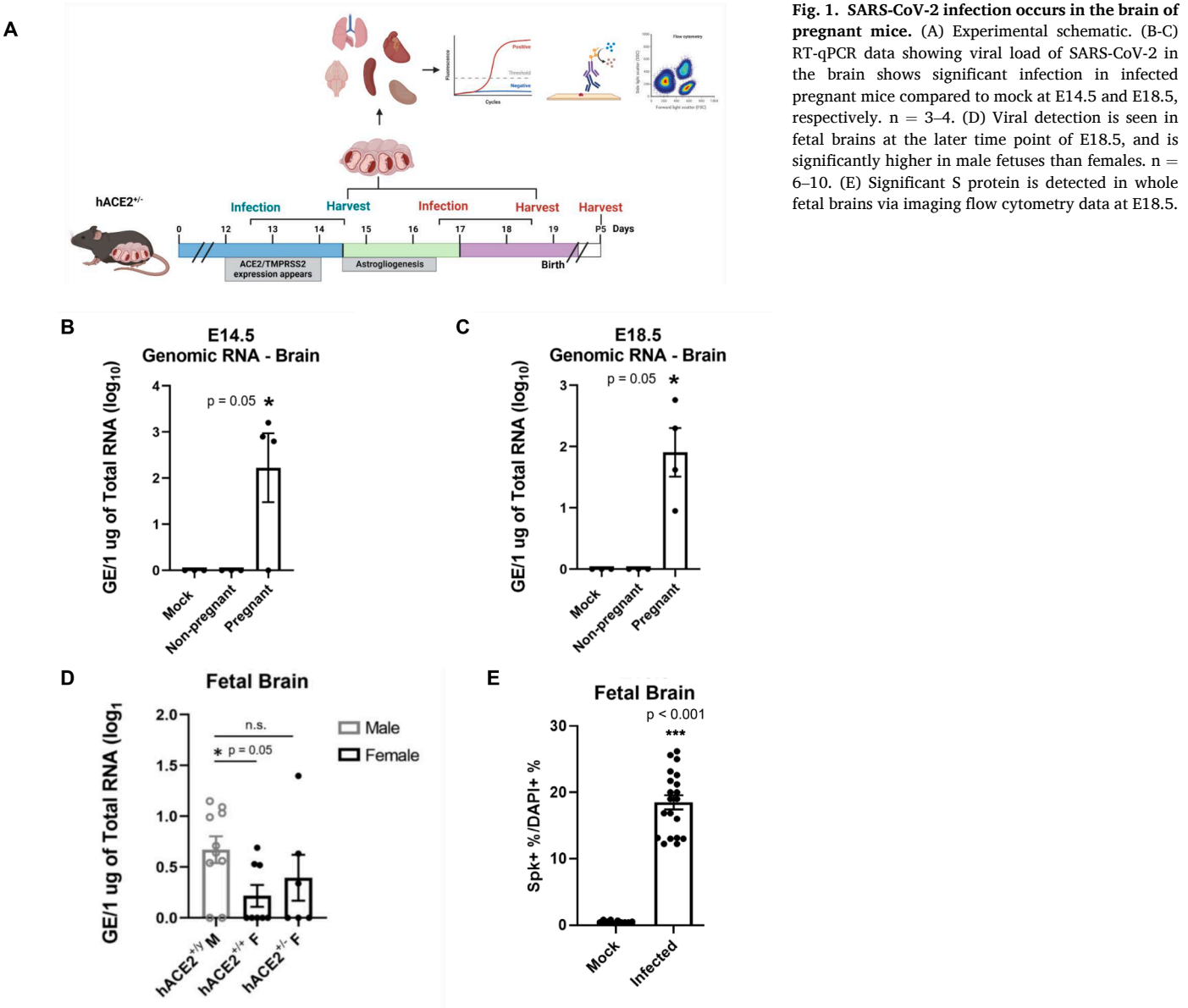

Fig. 1. SARS-CoV-2 infection occurs in the brain of pregnant mice. (A) Experimental schematic. (B-C) RT-qPCR data showing viral load of SARS-CoV-2 in the brain shows significant infection in infected pregnant mice compared to mock at E14.5 and E18.5, respectively. n = 3–4. (D) Viral detection is seen in fetal brains at the later time point of E18.5, and is significantly higher in male fetuses than females. n = 6–10. (E) Significant S protein is detected in whole fetal brains via imaging flow cytometry data at E18.5.

developmental stage in pregnant mice, which were infected at one of two time points (Fig. 1A). In order to determine if astrocyte emergence affected infection levels in the fetal brain, as hypothesized due to data from our previous study (McMahon et al. 2021), the first time point was at the mid-gestational stage of E12.5, which occurred following the initiation of ACE2/TMPRSS2 expression and prior to astrogliogenesis. This time point approximately matches the end of the first trimester and start of the second trimester in humans. The second time point was a late gestational stage that occurred post-astrogliogenesis and approximately matched early third trimester in humans. Both time points occur after placental formation, with fetal and maternal tissue harvesting at 48 hpi for analysis. Body weights of pregnant mice were used as a clinical sign of disease and were monitored post infection at both time points (Fig. S3). Infection at E12.5 resulted in a gain of 3.25 g (g) less than mock-infected mice on average, while infection at E16.5 resulted in a gain of 3.25 to 6 compared to mock-infected mice, despite rapid fetal growth at this gestational point. Additionally, infected mice displayed increased fur ruffling and hunched posture compared to mock-infected mice.

RT-qPCR analysis of the maternal lung at both time points showed similar levels of viral infection and replication in both pregnant and nonpregnant mice (Fig. S4). Genomic viral RNA was used to determine overall viral load in the lungs (Fig. S4A-B) and subgenomic viral mRNA levels, which indicate active transcription, was used as an indicator for viral replication (Fig. S4C, D). There were also similar viral loads detected in the spleens of both pregnant and nonpregnant mice at both time points, but no viral replication was observed in this tissue (Fig. S5). Interestingly, viral infection was detected at significant levels in the brains of pregnant mice at both time points, while none was detected in the brains of nonpregnant mice (Fig. 1B, C). Viral replication was not observed in the brains however (Fig. S6). The increased viral dissemination from the lungs to the brain, as well as increased weight loss suggests that pregnancy facilitates more invasive viral infection than in nonpregnant mice.

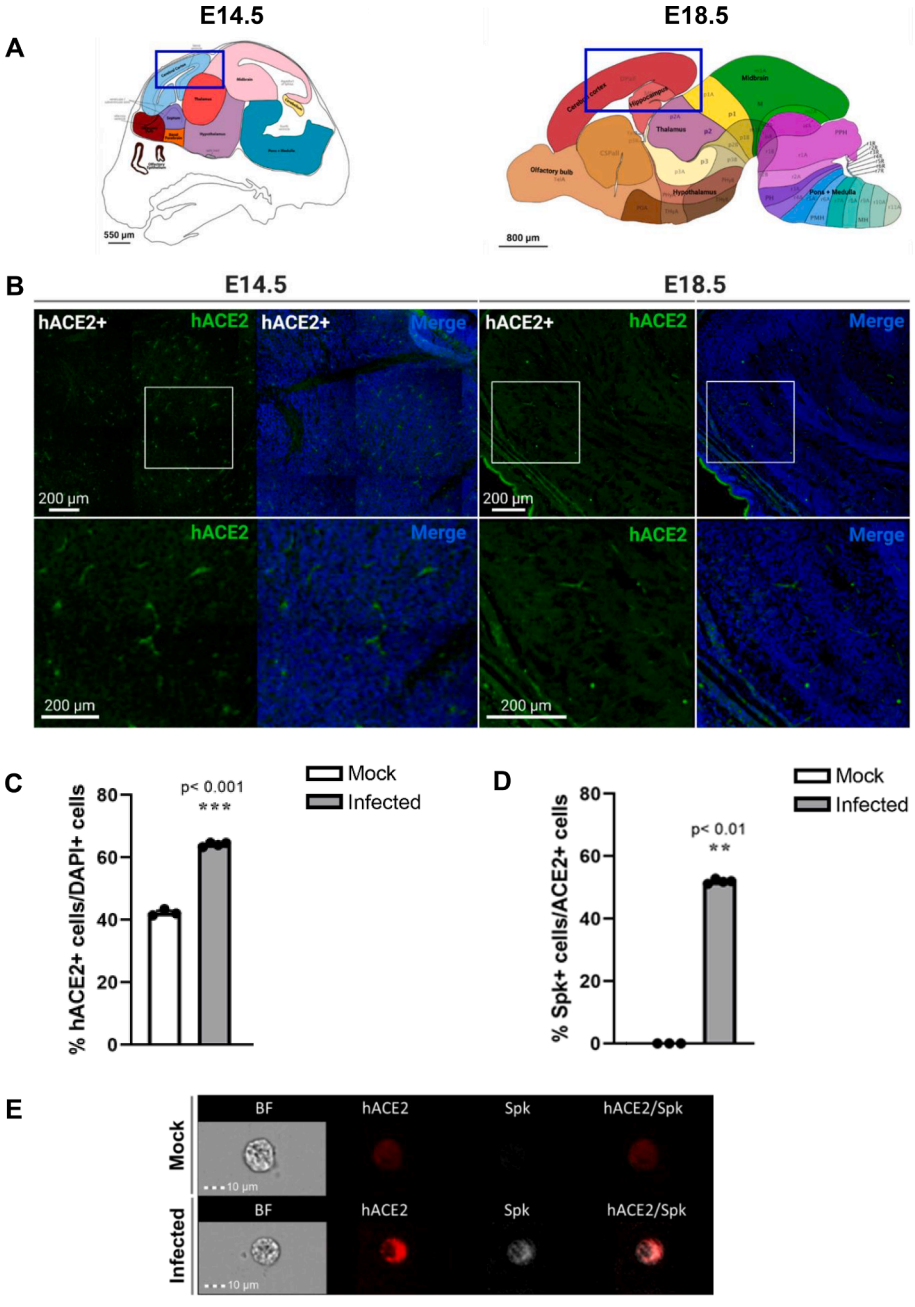

Fig. 2. hACE2 is seen in hACE2+ fetal mouse brains at both time points. (A) Allen brain atlas images of E15.5 and E18.5 fetal brains showing regions imaged for IHC (blue box). (B) hACE2 is detected in imaged regions of both E14.5 and E18.5 hACE2+ fetal brains. (C) Imaging flow cytometry of hACE2 expression in DAPI+ cells of mock-infected and infected fetal brains. (D) Imaging flow cytometry of S protein detection in hACE2+ cells. n = 4. (E) Representative images from imaging flow cytometry. (For interpretation of the references to color in this figure legend, the reader is referred to the web version of this article.)

3.3. SARS-CoV-2 infection occurs in hACE2 + but not hACE2- fetal tissues, including the fetal brain

RT-qPCR was conducted to evaluate viral load in infected hACE2+ and hACE2- fetal tissues at E14.5 and E18.5. At E14.5, only 22% of hACE2+ fetuses had positive detection for SARS-CoV-2 in abdominal, thoracic, and cardiac tissues (Fig. S7A), while over 60% of hACE2+ fetuses had positive detection in these tissues at E18.5 (Fig. S7B). Interestingly, of the 60% showing positive SARS-CoV-2 detection, 62% were males. Notably, there was no increase in infection amongst homozygous female fetuses compared to heterozygous fetuses. In the hACE2+ fetal brains, only 5% of fetuses had viral detection at E14.5 (Fig. S7C), and 58% had detection at E18.5 (Fig. 1D). Again, detection occurred primarily in males in the fetal brain at E18.5. Viral replication was not detected in any fetal tissues at either time point, however. Virus was also not detected in any tissues of the hACE2- fetuses (Fig. S8A–D).

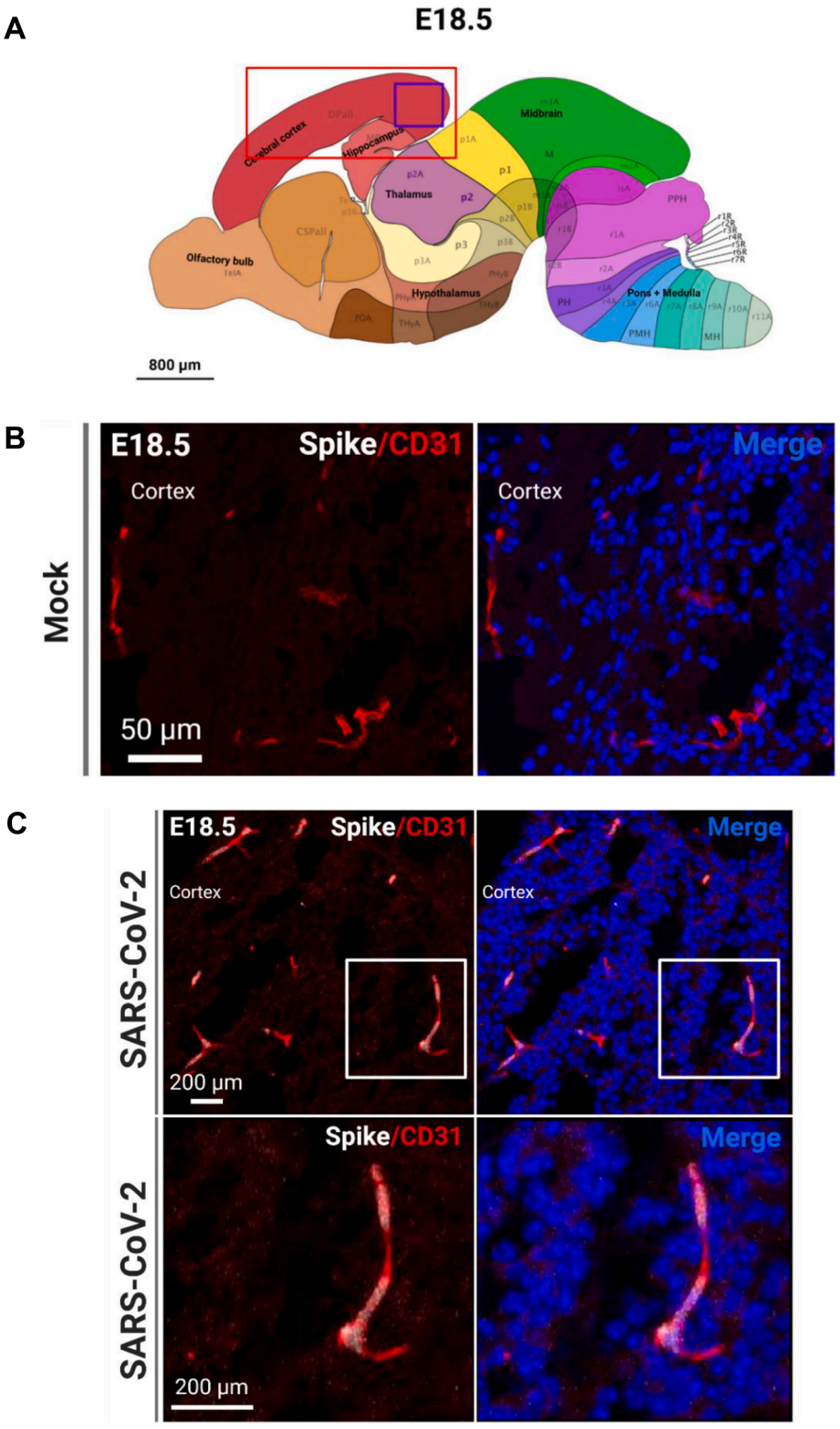

Fig. 3. SARS-CoV-2 infects endothelial cells in the fetal brain. (A) Allen brain atlas images showing regions of the brain analyzed for IHC (red box) and region shown in representative confocal image (purple box). (B) Representative image of CD31+ blood vessels in the mock-infected fetal brain. (C) Representative image of CD31+ and S protein+ blood vessels in the infected fetal brain. (For interpretation of the references to color in this figure legend, the reader is referred to the web version of this article.)

Along with RT-qPCR quantification, relative infection rates and distribution of infection were further analyzed through imaging flow cytometry. As shown by imaging flow cytometry data in Fig. 1E, 12–27% of cells from whole hACE2+ fetal brains had positive detection of SARS-CoV-2 S protein. Similar to the RT-qPCR data of whole fetal brains in Fig. 1D, there are two distinct populations of cells from infected fetuses.

Since SARS-CoV-2 was detected in the fetal brains, human ACE2 expression was evaluated in the brains at E14.5 and E18.5, the equivalent of 48 hpi in infection studies (Fig. 2). Immunohistochemistry of sagittal sections of the cortical and hippocampal regions of hACE2+ fetal brains showed hACE2 expression at both time points (Fig. 2A, B). To validate the antibody and confirm that non-specific binding was not occurring, IHC was conducted in hACE2- fetal tissues at E18.5 to confirm that hACE2 was not detected (Fig. S8E). Imaging flow cytometry was conducted by randomly sampling 50,000 dissociated cells from whole mock-infected and infected fetal brains (Fig. 2C–E). This data showed

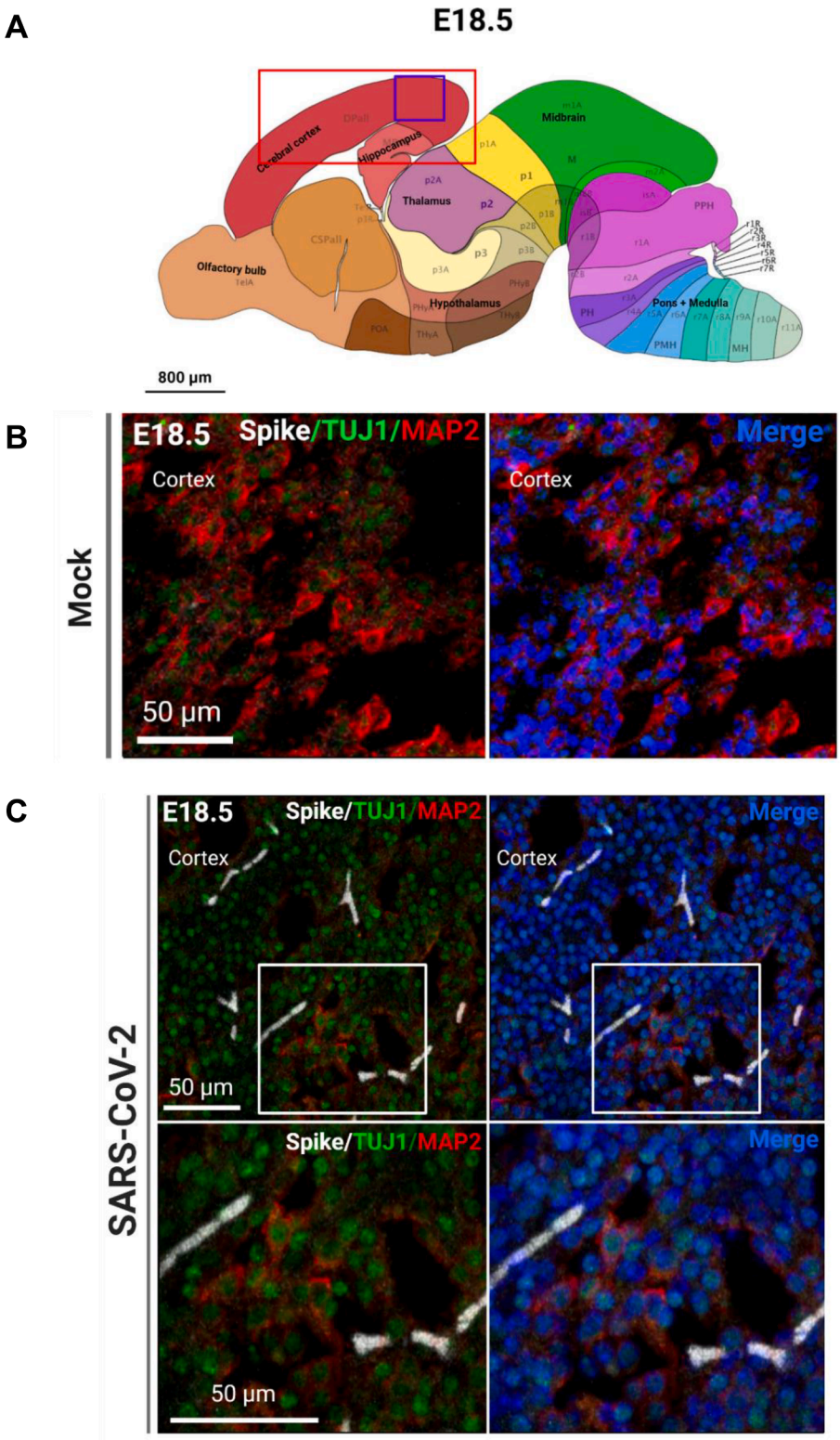

Fig. 4. SARS-CoV-2 infection surrounds neurons *in vivo*. (A) Allen brain atlas images showing regions of the brain analyzed for IHC (red box) and region shown in representative confocal image (purple box). (B) Representative confocal image of immature neuron marker TUJ1, and mature neuron marker MAP2 in the mock-infected fetal brain. (C) Representative images of SARS-CoV-2 S protein, immature neurons, and mature neurons in the infected fetal brain. (For interpretation of the references to color in this figure legend, the reader is referred to the web version of this article.)

that hACE2 expression was detected in ~ 40% of total sampled cells from mock-infected fetal brains, but in ~ 65% of cells from infected fetal brains (Fig. 2C). This supports data from our previous studies in organoids showing that ACE2 expression increases in neural tissue following SARS-CoV-2 infection (McMahon et al. 2021). Interestingly, several reports have found increased ACE2 levels in COVID-19 patients, speculating that circulating ACE2 ectodomain may assist in clearing or preventing infection spread by acting as a soluble decoy or limiting inflammation (Ciaglia, Vecchione, and Puca 2020; Nagy et al. 2021; Patel et al. 2021; Gutiérrez-Chamorro et al. 2021). Of the cells expressing hACE2 in infected fetal brains, ~50% of these also showed positive SARS-CoV-2 S protein detection, while there was no detection of S protein in the mock-infected fetal brains (Fig. 2D, E). Furthermore, SARS-CoV-2 S protein was not detected in hACE2- fetal brains through IHC (Fig. S8E). These data indicate that hACE2 is the receptor facilitating SARS-CoV-2 infection in this model system.

3.4. SARS-CoV-2 targets various cell types of the fetal brain at 48 hpi

Because of the significant viral detection in the fetal brains at E18.5, we conducted subsequent analyses at this time point. In order to determine the tropism of SARS-CoV-2 in the brain, we first conducted IHC to identify SARS-CoV-2 localization. Using the S protein as a marker for viral infection, we performed confocal imaging of the cortical and hippocampal regions of the fetal brain (Fig. 3A) and observed that the S protein appeared to be localizing within blood vessels of the brain. To ensure that the detected S protein signal was not due to autofluorescence, IHC was conducted for S protein detection in hACE2- fetal brains from infection groups (Fig. S8E) and in mock infected fetal brains (Fig. S9). No S protein detection was observed in these fetuses. For all

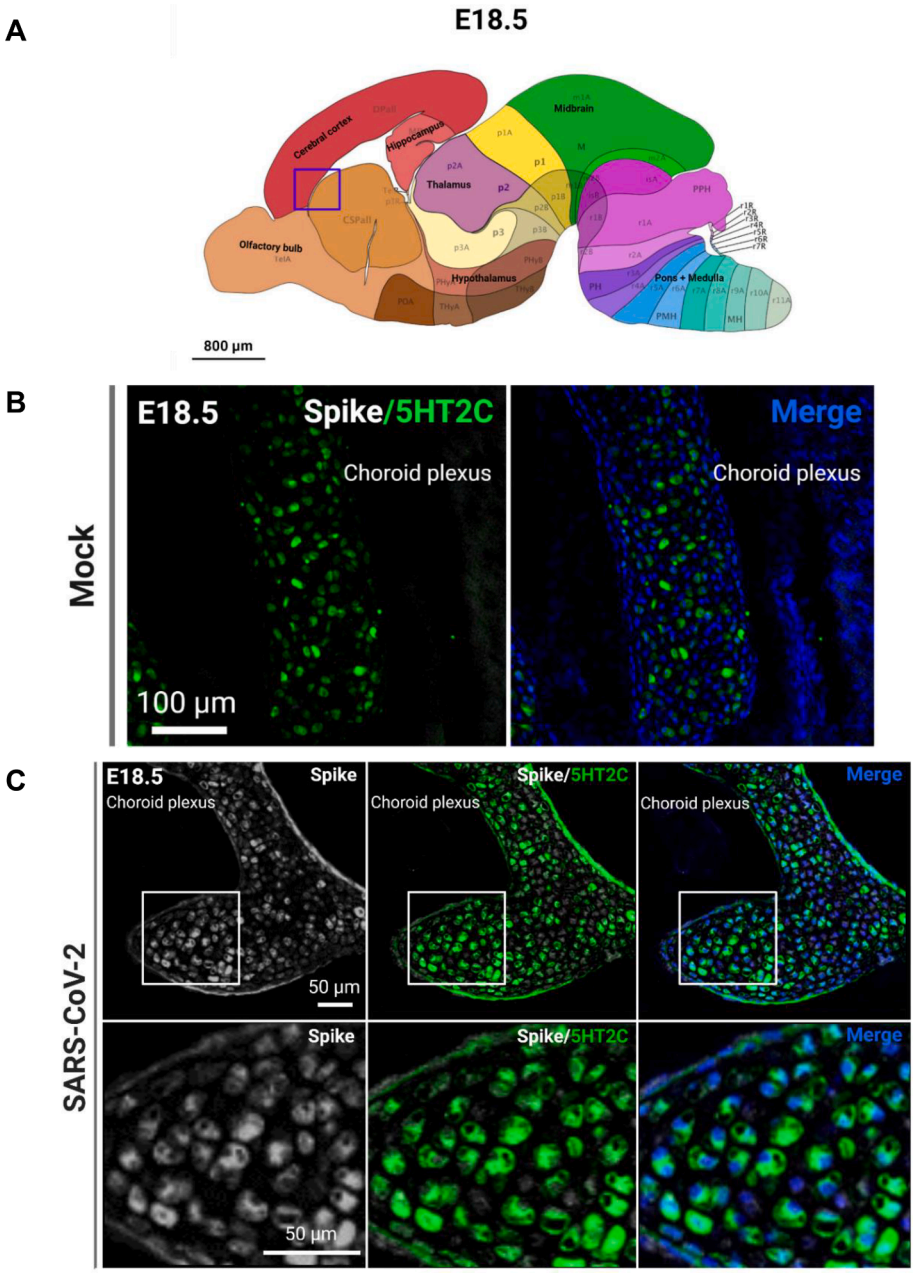

Fig. 5. SARS-CoV-2 infects ChP cells. (A) Region shown in representative confocal image (purple box). (B) Representative image of ChP marker 5HT2C in the mock-infected fetal brain. (C) SARS-CoV-2 S protein+ and 5HT2C+ ChP cells in infected fetal brain. (For interpretation of the references to color in this figure legend, the reader is referred to the web version of this article.)

subsequent IHC, mock-infected brains were stained for S protein and the respective cell type marker. To confirm blood vessel infection, we used CD31 to stain for endothelial cells in the brain and found co-localization of S protein with CD31 (Fig. 3B, C). The S protein was also detected in clusters within the blood vessels. Together, these data may suggest that SARS-CoV-2 enters the fetal brain through the circulatory system, also offering a method of viral transmission from mother to fetus. Next, we evaluated whether SARS-CoV-2 infection was found in other cells of the brain. As a marker for immature neurons, beta-3 tubulin (TUJ1) was used, and as a marker for mature neurons, MAP2 was used. We did not observe co-localization of S protein with TUJ1 or MAP2 in confocal images of sagittal sections of the fetal brain (Fig. 4C), which may be attributed to imaging only a few thin sections of a small region of the fetal brain (the cortex). To corroborate data from ours (McMahon et al. 2021) and other previous studies, we used 5HT2C as a marker for ChP cells. IHC showed co-localization with 5HT2C (Fig. 5A–C), suggesting that SARS-CoV-2 infects ChP cells in the fetal brain. Our previous data also found that SARS-CoV-2 infects astrocytes in human cortical organoids, and so we used ALDH1L1 as a marker for astrocytes (Fig. 6C). IHC data showed co-localization of ALDH1L1+ cells with S protein signal, suggesting infection of astrocytes. These data are in support of our previous findings in organoids. Furthermore, we evaluated infection in microglia, a cell type not present in our organoid model, and our data shows co-localization of microglial marker Iba1 with S protein (Fig. 7), indicating that infection of microglia also occurred in the fetal brains. Overall, IHC showed that SARS-CoV-2 does infect various cell types of

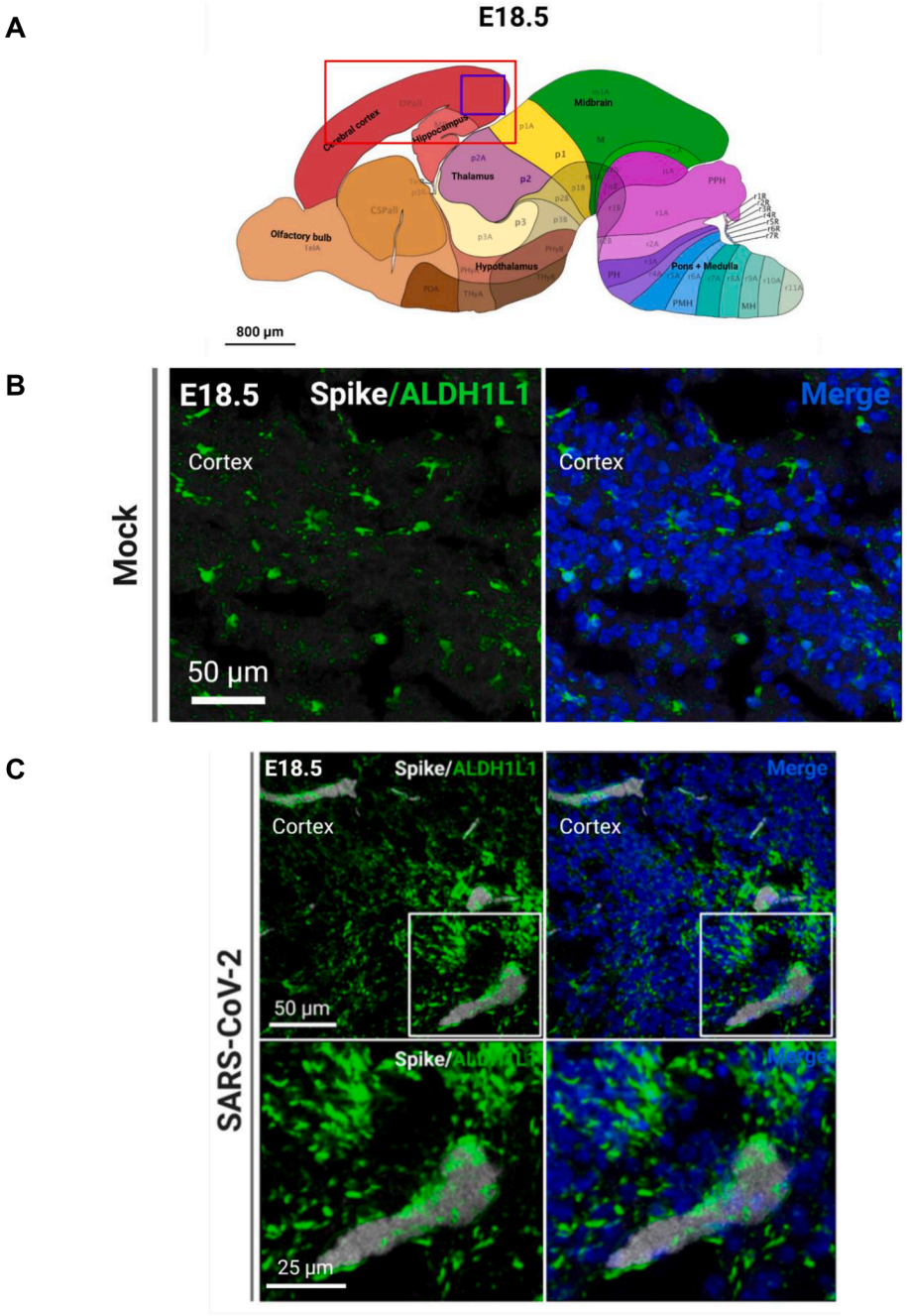

Fig. 6. SARS-CoV-2 infects astrocytes. (A) Regions of the brain analyzed for IHC (red box) and region shown in representative confocal image (purple box). (B) Representative image of astrocyte marker ALDH1L1 in the mock-infected fetal brain. (C) SARS-CoV-2 S protein+ and ALDH1L1+ astrocytes in the infected fetal brain. (For interpretation of the references to color in this figure legend, the reader is referred to the web version of this article.)

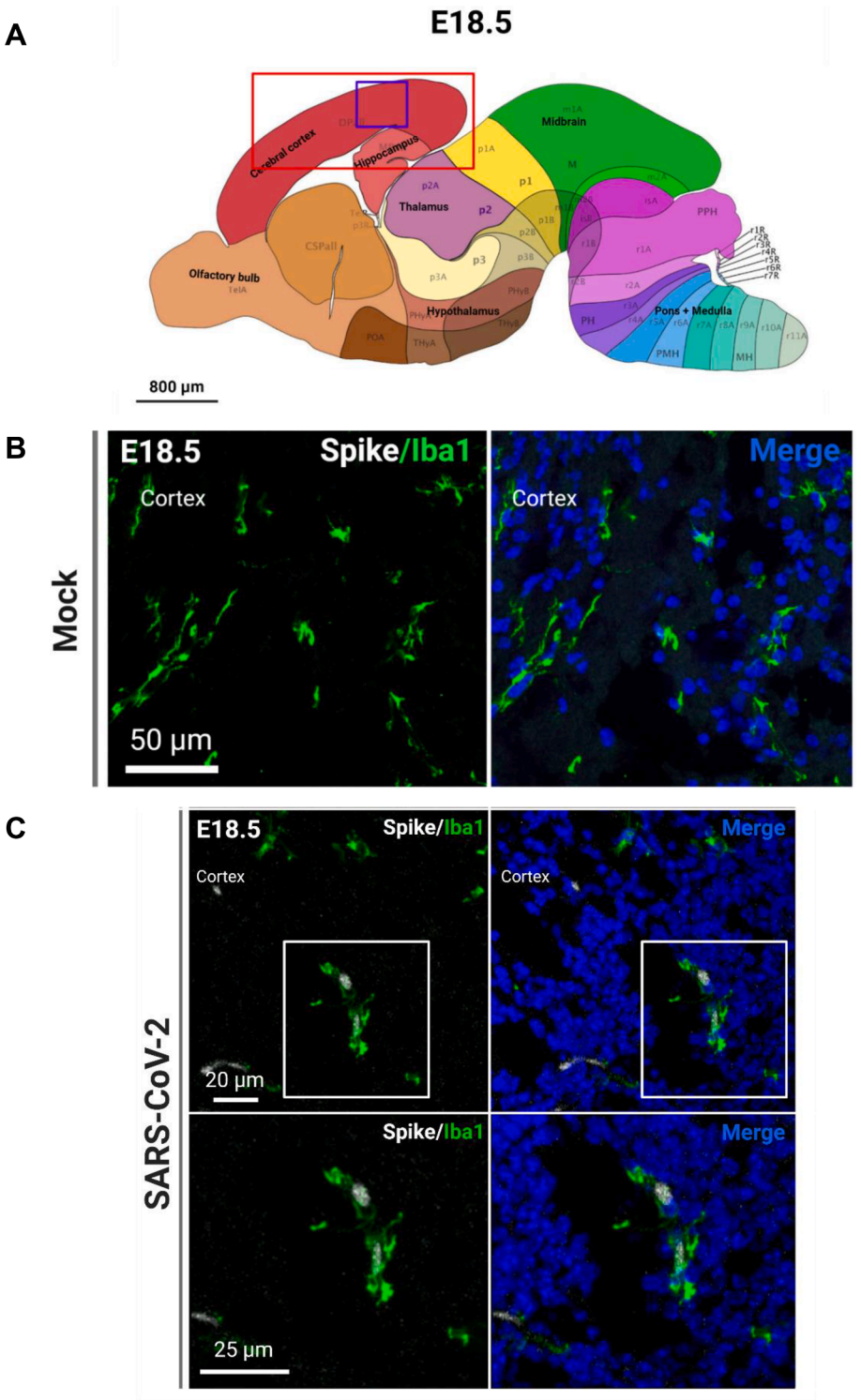

Fig. 7. SARS-CoV-2 infects microglia. (A) Regions of the brain analyzed for IHC (red box) and region shown in representative confocal image (purple box). (B) Representative image of microglia marker Iba1 in the mock-infected fetal brain. (C) SARS-CoV-2 S protein+ and Iba1+ microglia in the infected fetal brain. (For interpretation of the references to color in this figure legend, the reader is referred to the web version of this article.)

the fetal brain within 48 hpi.

Due to the inconclusive IHC data regarding neuronal infection by SARS-CoV-2, and to confirm the infection of other cell types in our IHC, we then used imaging flow cytometry (IFC) as a more sensitive method in order to closer evaluate infection at an individual cell level (Fig. 8). This also allowed us to obtain quantitative viral tropism data. To do this, we dissociated whole brains from both mock-infected and infected fetuses, then gated on single cells for mock-infected fetuses, or single cells that contained virus for samples from infected fetuses (Fig. 8A). We randomly obtained 50,000 cells from each sample, and then determined the percentage of S protein+ cells that were also positive for each respective cell type marker. Interestingly, we found that amongst S protein+ cells, ~19% were TUJ1+ and ~ 13% were MAP2+, indicating that SARS-CoV-2 does infect neurons in the fetal brain (Fig. 8B, C).

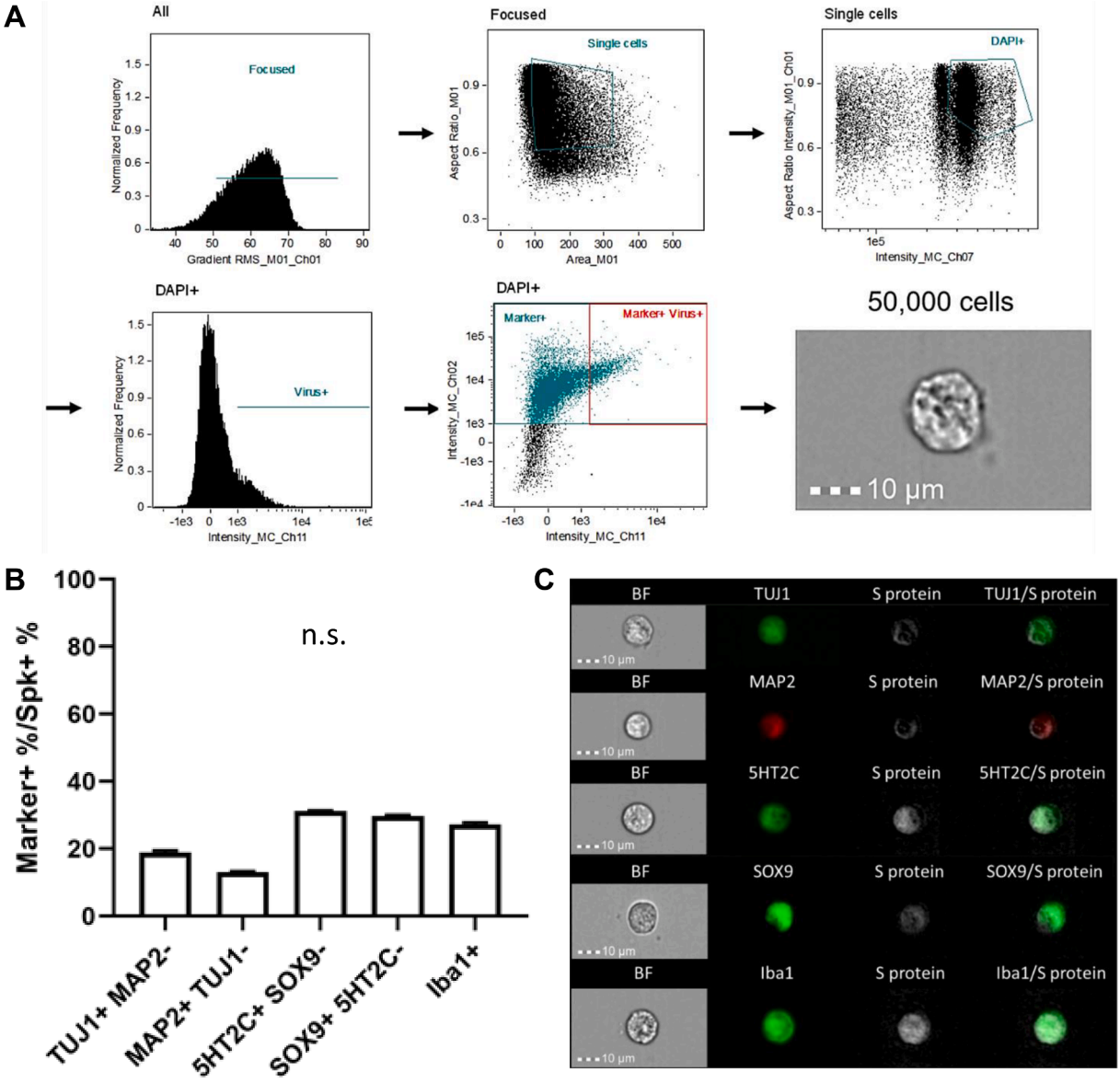

Fig. 8. SARS-CoV-2 infects various cells of the CNS. (A) Gating strategy to identify virus+ and marker+/virus+ cells for imaging flow cytometry. (B) Flow cytometry quantification of respective cell markers in S protein+ cells. n = 4. (C) Representative imaging flow cytometry images of infected cells from the fetal brain.

Confirming our IHC data and findings from previous studies, we found ChP marker, 5HT2C, detection in ~ 31% of infected cells. Using SOX9 as a marker for astrocytes in IFC, we confirmed that ~ 28% of infected cells were SOX9+, and found that approximately 27% of infected cells were also positive for our microglial marker, Iba1, further demonstrating that SARS-CoV-2 targets glial cells. Fig. S10 shows that S protein was not detected in mock-infected cells stained for each marker. Of note, percentages do not sum to 100% due to overlap of several markers in a portion of cells, such as TUJ1 and MAP2, and SOX9 and 5HT2C cells (Fig. 8B). Only co-localization of MAP2 with S protein was decreased compared to other cell types, however, there was less MAP2 expression in the fetal brain sections overall due to the early developmental time point of the fetal brain at E18.5 compared to later postnatal stages. Infection of neurons by SARS-CoV-2 is contrary to our previous findings, which were that SARS-CoV-2 only infects glial and ChP cells in human cortical organoids. Overall, our IFC data shows that SARS-CoV-2 can infect the various cell types of the fetal brain at similar levels within 48 h, suggesting that the fetal brain may be more susceptible to SARS-CoV-2 infection than previously thought.

3.5. SARS-CoV-2 does not cause changes in cell death levels at 48 hpi but promotes reactive gliosis at 7 dpi

We next investigated whether SARS-CoV-2 infection in these cells resulted in cell death at 48 hpi. We first conducted IHC using cleaved caspase-3 (aCasp3) as a marker for apoptotic cell death, and found no expression. We then conducted IFC using methods similar to the IFC in Fig. 8, and used Zombie aqua as an indicator for cell death. This data showed that cell death levels in infected fetal brains were comparable to levels from mock infection groups at 48 hpi (Fig. 9B). We hypothesized that increased cell death may instead occur at longer time points following infection, and we repeated IHC and imaging flow cytometry at 7 dpi. Again we found no expression of aCasp3 in IHC, and similarly found comparable cell death levels between mock and infected brains using Zombie yellow in IFC (Fig. 9D, E).

Because of this lack of change in cell death at both time points, we further investigated the consequences of infection on neurodevelopment by evaluating gliosis levels in the cortex and hippocampus at 7 dpi. GFAP and Iba1 expression were used as indicators for gliosis levels, and interestingly, both GFAP and Iba1 levels increased significantly in the

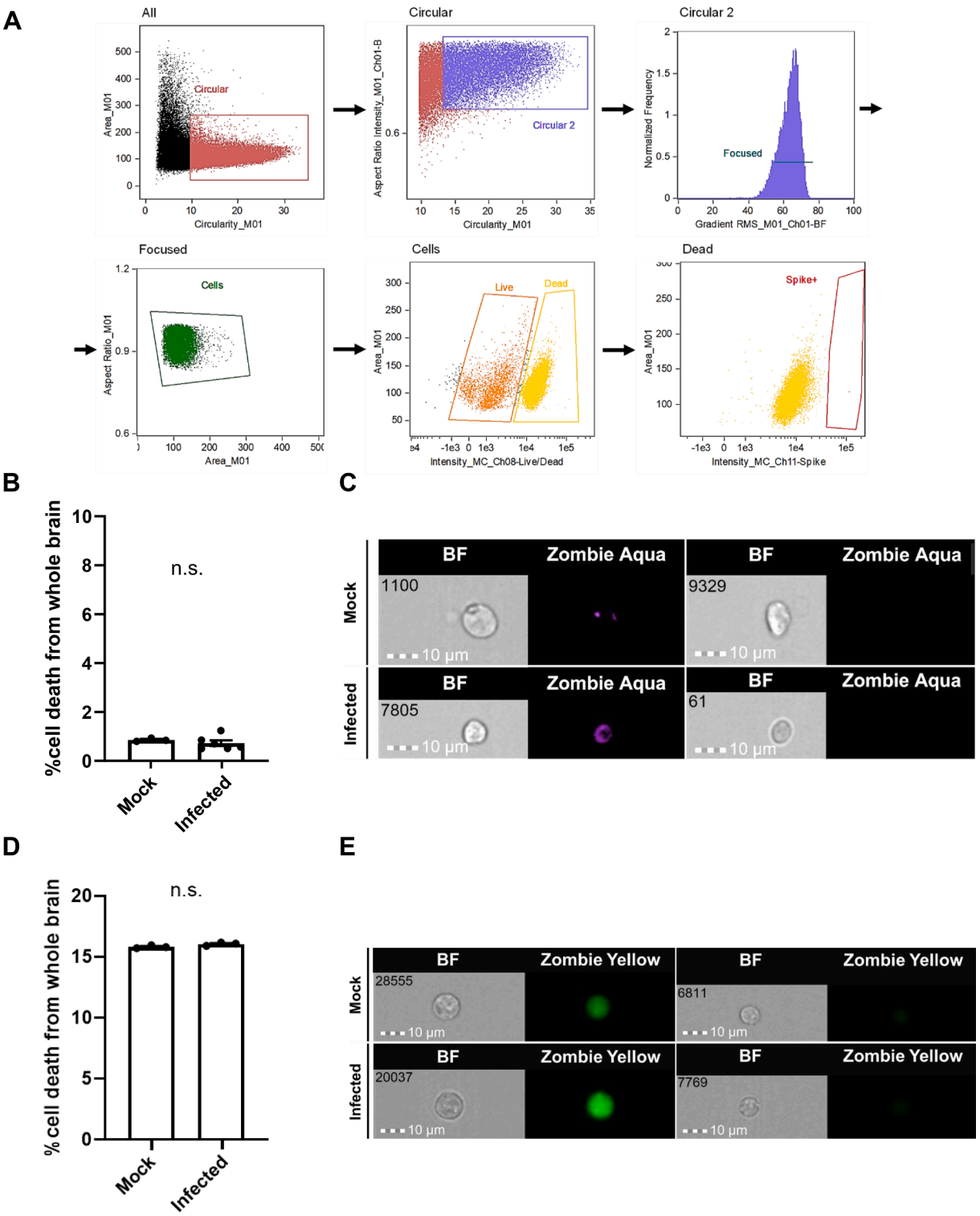

Fig. 9. Cell death levels are similar in mock and infected fetal brains at 48 hpi. (A) Gating schematic for imaging flow cytometry. (B) Flow cytometry quantification of cell death levels in whole mock-infected and infected fetal brains using Zombie aqua. n = 3–6 groups of 3 pooled samples (C) Representative imaging flow cytometry images. (D) Flow cytometry quantification of cell death levels in whole mock-infected and infected fetal brains at 7 dpi using Zombie yellow. n = 3 samples (E) Representative imaging flow cytometry images. (For interpretation of the references to color in this figure legend, the reader is referred to the web version of this article.)

brains of infected pups compared to mock-infected pups (Fig. 10A, B). GFAP-expressing astrocytes showed morphology typical of astrogliosis, with hypertrophic thicker processes and larger cell bodies, while microglia also developed "bushy" morphology with larger cell bodies, typical of reactive states (Fig. 10D, E). Of note, S protein was not detected at this time point, indicating that SARS-CoV-2 infection has cleared. Despite the lack of increased cell death and presence of virus, the finding and implications of increased gliosis as a result of infection during a critical point of neurodevelopment are of significant concern.

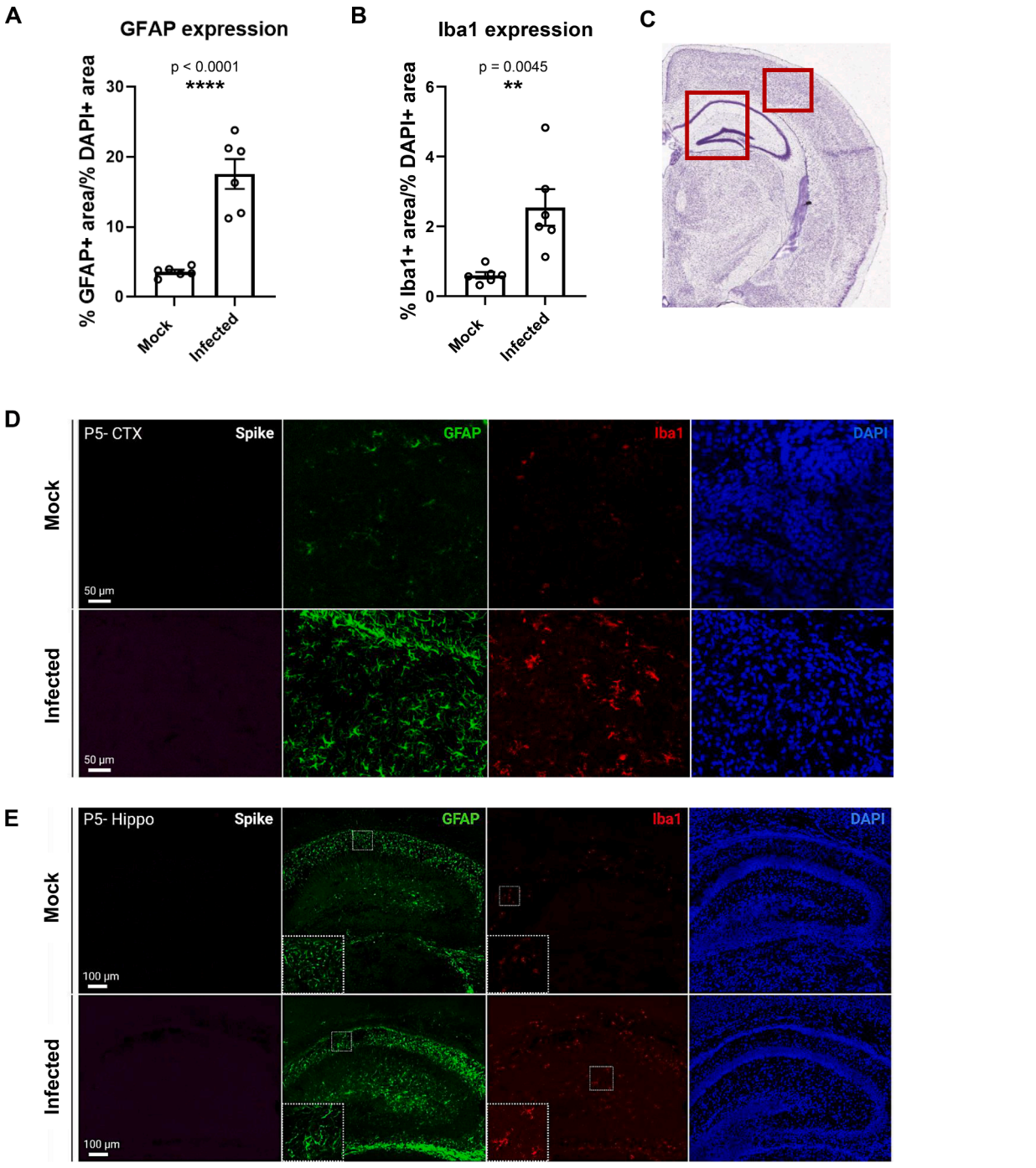

Fig. 10. Gliosis occurs in infected pups 7 dpi. (A) Quantification of the percent of GFAP expression over the percent of DAPI expression in 1 mm × 1 mm regions of fetal brain sections at 7 dpi. (B) Quantification of the percent of Iba1 expression over the percent of DAPI expression in 1 mm × 1 mm regions of fetal brain sections at 7 dpi. n = 6. (C) Regions of the brain shown in representative confocal image (red boxes). (D) Representative confocal images from the cortex of mock and infected P5 pups. (E) Representative confocal images from the hippocampus of mock and infected P5 pups. (For interpretation of the references to color in this figure legend, the reader is referred to the web version of this article.)

3.6. Maternal inflammation is not detected at 48 hpi, despite showing signs of disease

Because it is well established that the maternal immune response alone can cause neurodevelopmental effects in prenatally exposed offspring, we conducted ELISA assays to investigate whether maternal inflammation or the antiviral IFN response occurred following infection with SARS-CoV-2 (Fig. S11). We collected serum from both mock infection and experimental groups at 48 hpi. Interestingly, our data showed no change in inflammation at this time point in the infected groups compared to the mock infection groups (Fig. S11A, B), despite increased viral dissemination and significant weight loss in pregnant dams. Although we expected an increased IFN response after viral infection, we observed no difference in this viral-specific immune response amongst the groups (Fig. S11C, D).

3.7. Pre-term birth and early gross developmental differences are seen in infected compared to mock-infected litters

To further investigate the potential clinical significance of *in utero* SARS-CoV-2 exposure, we then evaluated the effects of infection on early gross development of the offspring. To do so, pregnant dams were infected at our later developmental time point of E16.5, then measurements of length and weight were conducted on separate groups of mock-infected and infected fetuses at E18.5 and neonates at P1 (Fig. S13). Notably, we observed pre-term birth in approximately 45% of infected litters. Neonates born before E19.5 were excluded from length and weight measurements for this experiment. At both time points, the infected group was significantly greater in length (Fig. S13A, B) and weight (Fig. S13C, D) than the mock-infected group. Together, this data suggests that *in utero* SARS-CoV-2 infection has consequences on early developmental of the body, and may persist later in life as a result of pre-term birth.

4. Discussion

Until recently, it was widely believed that SARS-CoV-2 did not cross from the mother to the developing fetus during a maternal case of COVID-19; however, evidence of neurodevelopmental deficits in neonates exposed *in utero* (de Medeiros et al. 2022; Jamieson and Rasmussen 2022; Rasmussen and Jamieson 2022; Liu et al. 2021; Archuleta et al. 2022; Aldrete-Cortez et al. 2022) and a more recent study looking at SARS-CoV-2 RNA in neonatal autopsy tissues (Reagan-Steiner et al. 2022) now suggests otherwise. One study in particular found that neonates exposed during the late second trimester to maternal COVID-19 had high levels of SARS-CoV-2 antibodies and displayed severe neurological complications, but did not test positive at birth via PCR for active COVID-19 infections (Benny et al. 2023). Furthermore, SARS-CoV-2 proteins were found in the placentas from these mothers, and after the sudden death of one of the infants at 13 months of age, SARS-CoV-2 detection was found in the brain. This suggests that vertical transmission of SARS-CoV-2 in humans can occur, and that direct infection of the brain can lead to ongoing neurological complications. Many viral pathogens such as Zika virus, HSV, HIV, and more are able to cross the placenta and infect fetal tissues, resulting in mild to severe neurological complications (Xu et al. 2020; Shapiro-Mendoza et al. 2017; Meertens et al. 2017; Coelho and Crovella 2017; Muldoon et al. 2020). A previous study that we conducted using human ESC-derived brain organoids demonstrated the infection capability of SARS-CoV-2 in developing brain tissue (McMahon et al. 2021), thus, we investigated the potential for SARS-CoV-2 transmission from mother to fetus at two different time points of development, as well as the tropism in the fetal brain in particular.

In this study, we confirmed that SARS-CoV-2 could be transmitted to the fetus at time points matching the second and third trimesters of human pregnancy using hACE2-KI mice (E12.5–14.5 and E16.5–18.5). Infection levels were much lower at a time point equivalent to the second trimester in humans, E12.5–14.5, but significant infection levels were observed at the third-trimester equivalent time point of E16.5–18.5. At this later time point, two distinct populations from infected fetal tissues were detected. While a lower population of infected cells was also detected using imaging flow cytometry, RT-qPCR data showed fetal brains without SARS-CoV-2 RNA. This discrepancy, as well as the lower infection levels at E14.5, may be due to deceased dissemination in some infected dams, as shown in Fig. S12. In addition, hACE2 expression levels were similar at both time points, further suggesting that this may be attributed to decreased viral dissemination in the mothers.

Interestingly, viral infection rates and levels were higher in males than in female fetuses. Further studies can be done to elucidate the role of sex in infection differences, as there are several possible explanations for our observations. For example, estrogen has been shown to act as a protective factor against various viral pathogens including SARS-CoV-2, while androgens have been correlated with increased vulnerability to SARS-CoV-2 infection (Mateus et al. 2022; Stárka and Dušková 2021; Magri et al. 2017; Wambier and Goren 2020; Al-Kuraishy et al. 2021). A proposed mechanism for this is that androgen receptor activation is necessary for TMPRSS2 transcription to occur and the gene loci for both ACE2 and androgen receptor is located on the X-chromosome, thus increased X-linked inheritance may lead to increased susceptibility to SARS-CoV-2 infection (Wambier and Goren 2020).

We also confirmed that in our model, hACE2 expression was necessary for SARS-CoV-2 infection. WT mice are typically not susceptible to SARS-CoV-2 binding and infection due to conformational differences in their ACE2 receptors compared to human ACE2, with one pre-print demonstrating a rare exception (Joyce et al. 2022). In humans, there are numerous receptors that have been found to bind SARS-CoV-2 and allow for productive infection (Gusev et al. 2022; Varma et al. 2020), and so ours is a conservative model for infection potential.

We then looked at the method of SARS-CoV-2 entry into the brain and SARS-CoV-2 tropism in neural tissue. We found that SARS-CoV-2 was primarily localized in blood vessels of the brain, indicating a potential transmission mechanism from mother to fetus via the circulatory system. This is consistent with studies from patient samples, in which systemic circulation as a primary means for SARS-CoV-2 transmission to the brain has been established in (Batta et al. 2021; Pillai et al. 2021). Infection of the endothelial cells is consistent with several *in vivo* studies which have found high ACE2 expression in this cell type, along with infection-induced damage of the vasculature (Batta et al. 2021; Varga et al. 2020; Ackermann et al. 2020). Of note, ACE2 expression within this cell type has been shown to differ in one study, which may be attributed to differences amongst *in vivo* and *in vitro* models between studies (McCracken et al. 2021). Furthermore, infection in additional cell types of the fetal brain such as neurons, glial cells, and ChP cells was observed in our mouse model within 48 h of infection, concordant with reports in human tissue (Gomes et al. 2021; Pellegrini et al. 2020; Jacob et al. 2020; Zhang et al. 2020; Andrews et al. 2022). Notably, neuronal infection was contrary to our previous studies using ESC-derived human neural organoids. This discrepancy may be due to limitations of our *in vitro* organoid model however, such as a lack of relevant cell types, receptors, and inflammatory pathways expressed.

Interestingly, we found a lack of viral replication in this study, despite the observed widespread infection amongst fetal brain cells. While inconclusive in our study, this may occur as a result of damage to the infected blood vessels by viral infection, as vascular damage has been widely reported in COVID-19 patients (Batta et al. 2021; Ackermann et al. 2020; Østergaard 2021), causing ruptures and leakage of viral particles via hemorrhagic dissemination from the mother's system. Future studies to investigate this further can be done by using dextran and a fluorophore-tagged SARS-CoV-2 variant to visualize leakage from the blood vessels and subsequent viral spreading, similar to studies done by Gibson et al. (Gibson et al. 2022). Furthermore, clustering of viral infected endothelial cells, as seen in our current data, can be used as evidence to exclude the possibility of spreading via passive viral transport through the blood, as this indicates a region of cellular infection and subsequent damage. To enhance visualization of viral clustering within blood vessels, whole mount staining enabling more 3D imaging of intact vessels can also be done.

Another enigmatic finding in our study was that cell death levels were comparable in the brains of both mock-infected and infected fetuses through IHC and imaging flow cytometry evaluation. A possible explanation was that our initial time point for tissue harvesting and analysis occurred at 48 hpi, which may not have been enough time for this process to occur at detectable levels. Thus, to further investigate this, experiments with longer end points were conducted to determine if cell death changes happen at 7 dpi; however, we also found similar levels of cell death in mock and infected brains at this time point. A possible explanation for the lack of increased cleaved caspase-3

detection in infected brains at both time points is that several studies have found that SARS-CoV-2 primarily induces the caspase 1-dependent cell death pathway of pyroptosis (Wang et al. 2022; Ferreira et al. 2021; Bittner et al. 2022; Sun et al. 2022). Pyroptosis may also explain the lack of increased cell death detection via IFC. Another possible explanation is that immune cell clearance of lysed cells may occur after 48 hpi but before 7 dpi, explaining the lack of viral detection at 7 dpi. Additionally, pyroptotic cells generate very low positive signals in cell death assays due to low levels of DNA fragmentation and integral nuclei (Yu et al. 2021; Wang et al. 2021).

Because pyroptosis is an inflammatory cell death mechanism (Bergsbaken, Fink, and Cookson 2009; Hsu et al. 2021), we then looked for alternate consequences of infection on neurodevelopment by evaluating gliosis via astrocyte and microglial activation. In the cortex and hippocampal regions of infected brains at 7 dpi, GFAP levels were significantly increased in astrocytes, which also displayed hypertrophic reactive morphology. Increased GFAP levels, as well as other indicators for astrogliosis, have been observed in the plasma and brain in post-mortem patient samples after COVID-19 and other viral infections (Tremblay et al. 2020; Issa et al. 2020; Li et al. 2018; Sahin et al. 2022) and following traumatic brain injuries (TBIs), making GFAP a reliable biomarker for brain injury and dysfunction (Bazarian et al. 2018; Moseby-Knappe et al. 2021; Yue et al. 2020). Previous literature has also reported high expression of GFAP in the brains of individuals with Autism Spectrum Disorder (ASD) compared to healthy controls, suggesting that some effects of gliosis during early development may even persist later in life (Abdelli, Samsam, and Naser 2019).

Similarly, when evaluating microglial activation in these regions, we found increased Iba1 levels with bushy, reactive morphology. Sustained or chronic microglial activation, or even activation during critical developmental stages in the brain can lead to lasting damage such as impaired memory and altered neuronal plasticity (Muzio, Viotti, and Martino 2021; Gogoleva, Drutskaya, and Atretkhany 2019), with viral infection at any stage of life being a major cause of gliosis (Bilbo et al. 2018; Ashraf et al. 2021; Fatemi et al. 2002). While gliosis is an essential protective process in the brain, it can lead to damaging levels of neuroinflammation when it occurs during crucial stages of early neurodevelopment, such as the P5 brain. As a result, neural structure and connectivity can be can be altered, leading to cognitive and behavioral deficits later in life (Abdelli, Samsam, and Naser 2019; Rhodes et al. 2004; Cardoso et al. 2015).

The findings of this study have vital implications for neurodevelopment. Infection-induced damage to the blood vessels can result in narrowing, ruptures, or leaks, which can lead to stroke or hemorrhage in the young or adult brain later in life (Østergaard 2021; Ackermann et al. 2020; Batta et al. 2021). In clinical studies, SARS-CoV-2 infection of the vasculature has been found to result in severe endothelial damage due to vascular thrombosis and weakening of endothelial cell membranes, as well as microangiopathy, leading to patient death (Ackermann et al. 2020). As previously mentioned, SARS-CoV-2 also infects other cells of the CNS, which can have significant implications for neurodevelopment as well. Other than neurons, glial and ChP cells are crucial for regulation of brain function, development, and immune response. Dysfunction of the choroid plexus has been associated with a variety of neurological disorders, to include aberrant development, neurodegeneration, and even autoimmune diseases (Mihaljevic et al. 2021). Glial cell dysfunction and gliosis have also been associated with a number of complications and disorders of the brain (Gao and Hernandes 2021; Vandenbark et al. 2021; Zhao et al. 2021). Our findings in this study give rise to the question of what functional effects, such as behavioral and cognitive alterations, does infection of the developing brain have later in life.

Three years into the pandemic, reports are now being made of neurodevelopmental deficits in babies exposed to COVID-19 during development (Aldrete-Cortez et al. 2022; Liu et al. 2021). Our findings may explain these clinical observations. Since it is well established that prenatal viral infection and inflammation exposure is strongly associated with behavioral abnormalities later in life (Tomonaga 2004; Tarr et al. 2012; Shi et al. 2003; Ronovsky et al. 2017; Hava et al. 2006; Fernández de Cossío et al. 2017; Carlezon et al. 2019; Baharnoori, Bhardwaj, and Srivastava 2012), and we have shown here that viral infection can quickly and efficiently disseminate to fetal tissues from the infected mother, leading to gliosis in the developing brain, this suggests that individuals infected *in utero* may be pre-disposed to the development of neuropsychiatric disorders at some point in their life. Our future studies aim to elucidate this. Overall, this study offers novel insight into COVID-19 infections of the brain and infection of the fetus, and may explain the deficits seen in neonates currently and disorders that arise in infected offspring in later years.

We also hypothesized that maternal inflammation during pregnancy could have effects on the development of the fetal brain, as it has been well noted in literature to result in neurological disorder development later in life (Burd, Balakrishnan, and Kannan 2012; Hava et al. 2006). To investigate this, we created a breeding scheme that allowed for litters containing both SARS-CoV-2-susceptible (hACE2+) and SARS-CoV-2-resistant (hACE2-) fetal genotypes. Since hACE2- fetuses were not susceptible to viral infection, alterations in neurodevelopment or function following a maternal COVID-19 infection could be attributed to exposure to maternal inflammation. Our data showed that at 48 hpi, there was no increase in inflammation or an IFN response in infected pregnant mice compared to mock-infected pregnant mice. Upregulation of many inflammatory cytokines may take several days, however, the IFN response, which is the typical antiviral immune response, generally increases soon after infection with many viral pathogens (Krämer et al. 2021; Sacco et al. 2022). Consistent with our findings, other reports from COVID-19 studies propose that SARS-CoV-2 counteracts the typical and initial viral detection and antiviral IFN responses (Blanco-Melo et al. 2020; Gutiérrez-Chamorro et al. 2021; Hadjadj et al. 2020). These studies did find an increased inflammatory response, though these findings were in human patients. Interestingly, our maternal mice still showed clinical signs of disease, with hunched posture, ruffling of fur, and significant weight loss, despite the lack of an increase in inflammation. These mice also have high viral loads with notable viral dissemination. Further studies are needed to investigate this lack of maternal inflammation during a case of COVID-19.

To investigate additional consequences of *in utero* SARS-CoV-2 infection, we evaluated differences in early gross development of mock infected versus infected offspring. We found significant increases in both length and weight of infected E18.5 fetuses and P1 neonates born at term. Viral infections during pregnancy are typically associated with lower birthrates, which may result in gross and neurodevelopmental consequences later in life (Richards et al. 2013). Clinical studies have shown a correlation with moderate to severe COVID-19 infection and low birthweight, but this was not seen in cases of mild infection (Dileep, ZainAlAbdin, and AbuRuz 2022; Wei et al. 2021; Piekos et al. 2022). Alternatively, less severe COVID-19 infections during pregnancy were associated with fetal macrosomia, or higher birthweights (Simon et al. 2022), similar to the observations in our study. We also observed preterm birth in approximately 45% of infected dams, corroborating additional birth outcomes observed in women with COVID-19 infection during pregnancy (Piekos et al. 2022; Dileep, ZainAlAbdin, and AbuRuz 2022).

All together, the higher birth weights observed in infected litters, indicative of early gross developmental differences, and the neurological changes we observed are suggestive of downstream developmental effects. Later studies will be conducted to investigate the persistence of these developmental differences into adulthood, and the consequences of these neurological observations on cognition and behavior. Furthermore, we used the delta variant of SARS-CoV-2 in this study due to the high rate of neurological symptoms and infections associated with this variant, as well as its prevalence at the start of this study. While studies elucidating the effects seen following prenatal exposure to the more

recent and milder omicron variant are still needed, these findings are of great importance to those affected by the delta variant wave.

5. Conclusion

In the current study, our results demonstrate that a COVID-19 infection during pregnancy causes more severe disease in the mother, with increased viral dissemination compared to a non-pregnant state. Furthermore, SARS-CoV-2 transmission from mother to fetus does occur during later stages of gestation, possibly through the circulatory system. In the fetal brain, we found that SARS-CoV-2 infects blood vessels, neurons, glial cells, and cells of the choroid plexus, and leads to an increase in gliosis even after viral clearance. Early developmental differences were also observed between groups. Future studies are needed to evaluate why viral replication and increases in infection-induced cell death do not occur, however. Altogether, our findings suggest that a prenatal case of COVID-19 may have critical implications for neurodevelopment and function in the offspring. Our mouse model is conservative, and so our findings also suggest that the consequences on neurodevelopment may be more severe in humans, having higher natural susceptibility to SARS-CoV-2 infection than mice.

Declaration of Competing Interest

The authors declare that they have no known competing financial interests or personal relationships that could have appeared to influence the work reported in this paper.

Data availability

Data will be made available on request.

Acknowledgments

We thank Jake Lehle, Lorena Roa de la Cruz, Kaira Church, Sandra Cardona from the UTSA Cell Analysis Core, and Abby Ibarra and Miguel Angel Torres Martinez from the UTSA Laboratory Animal Resource Center for experimental logistics and technique assistance. This work was supported in part by the Stem Cell Core at the University of Texas at San Antonio and by grants from the NIH (U01DA054170 and R01NS113516 (to J.H.); and F31NS125966 (to C.L.M); San Antonio Partnership for Precision Therapeutics (SPN 01116); the Robert J. Kleberg, Jr. and Helen C. Kleberg Foundation; and the Semmes Foundation, Inc. Some figures were created with BioRender.com.

Appendix A. Supplementary data

Supplementary data to this article can be found online at https://doi.org/10.1016/j.bbi.2023.06.015.

References

Abdelli, L.S., Samsam, A., Naser, S.A., 2019. Propionic acid induces gliosis and neuroinflammation through modulation of PTEN/AKT pathway in autism spectrum disorder. Sci. Rep. 9, 8824.

Ackermann, M., Verleden, S.E., Kuehnel, M., Haverich, A., Welte, T., Laenger, F., Vanstapel, A., Werlein, C., Stark, H., Tzankov, A., Li, W.W., Li, V.W., Mentzer, S.J., Jonigk, D., 2020. Pulmonary Vascular endothelialitis, thrombosis, and angiogenesis in covid-19. N. Engl. J. Med. 383, 120–218.

Aldrete-Cortez, V., Bobadilla, L., Tafoya, S.A., Gonzalez-Carpinteiro, A., Nava, F., Viñals, C., Alvarado, E., Mendizabal-Espinosa, R., Gómez-López, M.E., Ramirez-Garcia, L.A., Perez-Miguel, A., Crovetto, F., 2022. Infants prenatally exposed to SARS-CoV-2 show the absence of fidgety movements and are at higher risk for neurological disorders: a comparative study. PLoS One 17 (5), e0267575.

al-Haddad, B.J.S., Oler, E., Armistead, B., Elsayed, N.A., Weinberger, D.R., Bernier, R., Burd, I., Kapur, R., Jacobsson, B.o., Wang, C., Mysorekar, I., Rajagopal, L., Adams Waldorf, K.M., 2019. The fetal origins of mental illness. Am. J. Obstet. Gynecol. 221 (6), 549–562.

Al-Kuraishy, H.M., Al-Gareeb, A.I., Faidah, H., Al-Maiahy, T.J., Cruz-Martins, N., Batiha, G.E., 2021. The looming effects of estrogen in covid-19: a rocky rollout. Front. Nutr. 8, 649128.

An, D., Li, K., Rowe, D.K., Diaz, M.C.H., Griffin, E.F., Beavis, A.C., Johnson, S.K., Padykula, I., Jones, C.A., Briggs, K., Li, G., Lin, Y., Huang, J., Mousa, J., Brindley, M., Sakamoto, K., Meyerholz, D.K., McCray, P.B., Tompkins, S.M., He, B., 2021. Protection of K18-hACE2 mice and ferrets against SARS-CoV-2 challenge by a single-dose mucosal immunization with a parainfluenza virus 5-based COVID-19 vaccine. Sci. Adv. 7 (27).

Andrews, M.G., Mukhtar, T., Eze, U.C., Simoneau, C.R., Ross, J., Parikshak, N., Wang, S., Zhou, L., Koontz, M., Velmeshev, D., Siebert, C.V., Gemenes, K.M., Tabata, T., Perez, Y., Wang, L., Mostajo-Radji, M.A., de Majo, M., Donohue, K.C., Shin, D., Salma, J., Pollen, A.A., Nowakowski, T.J., Ullian, E., Kumar, G.R., Winkler, E.A., Crouch, E.E., Ott, M., Kriegstein, A.R., 2022. Tropism of SARS-CoV-2 for human cortical astrocytes. PNAS 119, e2122236119.

Arbour, N., Day, R., Newcombe, J., Talbot, P.J., 2000. Neuroinvasion by human respiratory coronaviruses. J. Virol. 74, 8913–8921.

Archuleta, C., Wade, C., Micetic, B., Tian, A., Mody, K., 2022. 'Maternal COVID-19 infection and possible associated adverse neurological fetal outcomes. Two Case Reports', *Am J Perinatol* 39, 1292–2128.

Ashraf, U., Ding, Z., Deng, S., Ye, J., Cao, S., Chen, Z., 2021. Pathogenicity and virulence of Japanese encephalitis virus: neuroinflammation and neuronal cell damage. Virulence 12 (1), 968–980.

Baharnoori, M., Bhardwaj, S.K., Srivastava, L.K., 2012. Neonatal behavioral changes in rats with gestational exposure to lipopolysaccharide: a prenatal infection model for developmental neuropsychiatric disorders. Schizophr. Bull. 38 (3), 444–456.

Baig, A.M., Khaleeq, A., Ali, U., Syeda, H., 2020. 'Evidence of the COVID-19 virus targeting the CNS: tissue distribution, Host-Virus Interaction, and Proposed Neurotropic Mechanisms'. ACS Chem. Neurosci 11 (7), 995–998.

Baron-Cohen, S., Ring, H.A., Wheelwright, S., Bullmore, E.T., Brammer, M.J., Simmons, A., Williams, S.C., 1999. Social intelligence in the normal and autistic brain: an fMRI study. Eur. J. Neurosci. 11, 1891–1898.

Barry 3rd, H., Bary Jr., H., 1961. Season of birth. an epidemiological study in psychiatry. Arch. Gen. Psychiatry 5, 292–300.

Batta, Y., King, C., Johnson, J., Haddad, N., Boueri, M., Haddad, G., 2021. Sequelae and comorbidities of COVID-19 manifestations on the cardiac and the vascular systems. Front. Physiol. 12, 748972.

Bazarian, J.J., Biberthaler, P., Welch, R.D., Lewis, L.M., Barzo, P., Bogner-Flatz, V., Gunnar Brolinson, P., Büki, A., Chen, J.Y., Christenson, R.H., Hack, D., Huff, J.S., Johar, S., Jordan, J.D., Leidel, B.A., Lindner, T., Ludington, E., Okonkwo, D.O., Ornato, J., Peacock, W.F., Schmidt, K., Tyndall, J.A., Vossough, A., Jagoda, A.S., 2018. Serum GFAP and UCH-L1 for prediction of absence of intracranial injuries on head CT (ALERT-TBI): a multicentre observational study. Lancet Neurol. 17 (9), 782–789.

Benny, M., Bandstra, E.S., Saad, A.G., Lopez-Alberola, R., Saigal, G., Paidas, M.J., Jayakumar, A.R., 2023. Maternal SARS-CoV-2, placental changes and brain injury in 2 neonates. Pediatrics 151 (5).

Bergsbaken, T., Fink, S.L., Cookson, B.T., 2009. Pyroptosis: host cell death and inflammation. Nat. Rev. Microbiol. 7, 99–109.

Bilbo, S.D., Block, C.L., Bolton, J.L., Hanamsagar, R., Tran, P.K., 2018. Beyond infection - maternal immune activation by environmental factors, microglial development, and relevance for autism spectrum disorders. Exp. Neurol. 299, 241–251.

Bittner, Z.A., Schrader, M., George, S.E., Amann, R., 2022. Pyroptosis and Its role in SARS-CoV-2 infection. Cells 11.

Blanco-Melo, D., Nilsson-Payant, B.E., Liu, W.C., Uhl, S., Hoagland, D., Møller, R., Jordan, T.X., Oishi, K., Panis, M., Sachs, D., Wang, T.T., Schwartz, R.E., Lim, J.K., Albrecht, R.A., tenOever, B.R., 2020. Imbalanced host response to SARS-CoV-2 drives development of COVID-19. Cell 181, 1036-45.e9.

Burd, I., Balakrishnan, B., Kannan, S., 2012. Models of fetal brain injury, intrauterine inflammation, and preterm birth. Am. J. Reprod. Immunol. 67, 287–294.

Cardoso, F.L., Herz, J., Fernandes, A., Rocha, J., Sepodes, B., Brito, M.A., McGavern, D. B., Brites, D., 2015. Systemic inflammation in early neonatal mice induces transient and lasting neurodegenerative effects. J. Neuroinflammation 12, 82.

Carlezon Jr., W.A., Kim, W., Missig, G., Finger, B.C., Landino, S.M., Alexander, A.J., Mokler, E.L., Robbins, J.O., Li, Y., Bolshakov, V.Y., McDougle, C.J., Kim, K.S., 2019. Maternal and early postnatal immune activation produce sex-specific effects on autism-like behaviors and neuroimmune function in mice. Sci. Rep. 9, 16928.

Ciaglia, E., Vecchione, C., Puca, A.A., 2020. COVID-19 Infection and Circulating ACE2 Levels: Protective Role in Women and Children. Front. Pediatr. 8, 206.

Coelho, A., Crovella, S., 2017. Microcephaly prevalence in infants born to zika virus-infected women: a systematic review and meta-analysis. Int. J. Mol. Sci. 18 (8), 1714.

Conde Cardona, G., Quintana Pájaro, L.D., Quintero Marzola, I.D., Ramos Villegas, Y., Moscote Salazar, L.R., 2020. Neurotropism of SARS-CoV 2: mechanisms and manifestations. J. Neurol. Sci. 412, 116824.

Crunfli, F., Carregari, V.C., Veras, F.P., Silva, L.S., Nogueira, M.H., Antunes, A., Vendramini, P.H., Valença, A.G.F., Brandão-Teles, C., Zuccoli, G.D.S., Reis-de-Oliveira, G., Silva-Costa, L.C., Saia-Cereda, V.M., Smith, B.J., Codo, A.C., de Souza, G.F., Muraro, S.P., Parise, P.L., Toledo-Teixeira, D.A., Santos de Castro Í, M., Melo, B.M., Almeida, G.M., Firmino, E.M.S., Paiva, I.M., Silva, B.M.S., Guimarães, R. M., Mendes, N.D., Ludwig, R.L., Ruiz, G.P., Knittel, T.L., Davanzo, G.G., Gerhardt, J. A., Rodrigues, P.B., Forato, J., Amorim, M.R., Brunetti, N.S., Martini, M.C., Benatti, M.N., Batah, S.S., Siyuan, L., João, R.B., Aventurato Í, K., Rabelo de Brito, M., Mendes, M.J., da Costa, B.A., Alvim, M.K.M., da Silva Júnior, J.R., Damião, L.L., de Sousa, I.M.P., da Rocha, E.D., Gonçalves, S.M., Lopes da Silva, L.H., Bettini, V., Campos, B.M., Ludwig, G., Tavares, L.A., Pontelli, M.C., Viana, R.M.M.,

Martins, R.B., Vieira, A.S., Alves-Filho, J.C., Arruda, E., Podolsky-Gondim, G.G., Santos, M.V., Neder, L., Damasio, A., Rehen, S., Vinolo, M.A.R., Munhoz, C.D., Louzada-Junior, P., Oliveira, R.D., Cunha, F.Q., Nakaya, H.I., Mauad, T., Duarte-Neto, A.N., Ferraz da Silva, L.F., Dolhnikoff, M., Saldiva, P.H.N., Farias, A.S., Cendes, F., Moraes-Vieira, P.M.M., Fabro, A.T., Sebollela, A., Proença-Modena, J.L., Yasuda, C.L., Mori, M.A., Cunha, T.M., Martins-de-Souza, D., 2022. 'Morphological, cellular, and molecular basis of brain infection in COVID-19 patients'. *PNAS* 119, e2200960119.

de Medeiros, K.S., Sarmento, A.C.A., Costa, A.P.F., Macêdo, L.T.A., da Silva, L.A.S., de Freitas, C.L., Simões, A.C.Z., Gonçalves, A.K., 2022. Consequences and implications of the coronavirus disease (COVID-19) on pregnancy and newborns: a comprehensive systematic review and meta-analysis. Int. J. Gynaecol. Obstet. 156, 394–405.

Dileep, A., ZainAlAbdin, S., AbuRuz, S., 2022. Investigating the association between severity of COVID-19 infection during pregnancy and neonatal outcomes. Sci. Rep. 12, 3024.

Elam, H. B., J. J. Donegan, J. Hsieh, and D. J. Lodge. 2022. 'Gestational buprenorphine exposure disrupts dopamine neuron activity and related behaviors in adulthood', *eNeuro*, 9.

Fatemi, S.H., Emamian, E.S., Sidwell, R.W., Kist, D.A., Stary, J.M., Earle, J.A., Thuras, P., 2002. Human influenza viral infection in utero alters glial fibrillary acidic protein immunoreactivity in the developing brains of neonatal mice. Mol. Psychiatry 7, 633–640.

Fernández de Cossío, L., Guzmán, A., van der Veldt, S., Luheshi, G.N., 2017. Prenatal infection leads to ASD-like behavior and altered synaptic pruning in the mouse offspring. Brain Behav. Immun. 63, 88–98.

Ferreira, A.C., Soares, V.C., de Azevedo-Quintanilha, I.G., Sdsg Dias, N., Fintelman-Rodrigues, C.Q., Sacramento, M., de Mattos, C.S., Freitas, J.R., Temerozo, L., Teixeira, E.D., Hottz, E.A., Barreto, C.R.R., Pão, L., Palhinha, M., Miranda, D.C., Bou-Habib, F.A., Bozza, P.T., Bozza, Souza, T.M.L., 2021. SARS-CoV-2 engages inflammasome and pyroptosis in human primary monocytes. Cell Death Discov 7, 43.

Flaherman, V.J., Afshar, Y., Boscardin, J., Keller, R.L., Mardy, A., Prahl, M.K., Phillips, C., Asiodu, I.V., Berghella, W.V., Chambers, B.D., Crear-Perry, J., Jamieson, D.J., Jacoby, V.L., Gaw, S.L., 2020. Infant outcomes following maternal infection with SARS-CoV-2: first report from the PRIORITY Study. Clin. Infect. Dis.

Gao, Q., Hernandes, M.S., 2021. Sepsis-associated encephalopathy and blood-brain barrier dysfunction. Inflammation 44, 2143–2150.

Gibson, J.F., Bojarczuk, A., Evans, R.J., Kamuyango, A.A., Hotham, R., Lagendijk, A.K., Hogan, B.M., Ingham, P.W., Renshaw, S.A., Johnston, S.A., 2022. Blood vessel occlusion by Cryptococcus neoformans is a mechanism for haemorrhagic dissemination of infection. PLoS Pathog. 18, e1010389.

Gogoleva, V.S., Drutskaya, M.S., Atretkhany, K.S., 2019. The role of microglia in the homeostasis of the central nervous system and neuroinflammation. Mol. Biol. (Mosk) 53, 790–878.

Gomes, I., Karmirian, K., Oliveira, J.T., Cdsg Pedrosa, M.A., Mendes, F.C., Rosman, L.C., Rehen, S., 2021. SARS-CoV-2 infection of the central nervous system in a 14-month-old child: a case report of a complete autopsy. Lancet Reg Health Am 2, 100046.

Gusev, E., Sarapultsev, A., Solomatina, L., Chereshnev, V., 2022. SARS-CoV-2-specific immune response and the pathogenesis of COVID-19. Int. J. Mol. Sci. 23.

Gutiérrez-Chamorro, L., Riveira-Muñoz, E., Barrios, C., Palau, V., Nevot, M., Pedreño-López, S., Senserrich, J., Massanella, M., Clotet, B., Cabrera, C., Mitjà, O., Crespo, M., Pascual, J., Riera, M., Ballana, E., 2021. SARS-CoV-2 infection modulates ACE2 function and subsequent inflammatory responses in swabs and plasma of COVID-19 patients. Viruses 13.

Hadjadj, J., Yatim, N., Barnabei, L., Corneau, A., Boussier, J., Smith, N., Péré, H., Charbit, B., Bondet, V., Chenevier-Gobeaux, C., Breillat, P., Carlier, N., Gauzit, R., Morbieu, C., Pène, F., Marin, N., Roche, N., Szwebel, T.A., Merkling, S.H., Treluyer, J.M., Veyer, D., Mouthon, L., Blanc, C., Tharaux, P.L., Rozenberg, F., Fischer, A., Duffy, D., Rieux-Laucat, F., Kernéis, S., Terrier, B., 2020. Impaired type I interferon activity and inflammatory responses in severe COVID-19 patients. Science 369, 718–724.

Hava, G., Vered, L., Yael, M., Mordechai, H., Mahoud, H., 2006. Alterations in behavior in adult offspring mice following maternal inflammation during pregnancy. Dev. Psychobiol. 48, 162–168.

Helms, J., Kremer, S., Merdji, H., Clere-Jehl, R., Schenck, M., Kummerlen, C., Collange, O., Boulay, C., Fafi-Kremer, S., Ohana, M., Anheim, M., Meziani, F., 2020. Neurologic Features in severe SARS-CoV-2 infection. N. Engl. J. Med. 382, 2268–2270.

Hsu, S.K., Li, C.Y., Lin, I.L., Syue, W.J., Chen, Y.F., Cheng, K.C., Teng, Y.N., Lin, Y.H., Yen, C.H., Chiu, C.C., 2021. Inflammation-related pyroptosis, a novel programmed cell death pathway, and its crosstalk with immune therapy in cancer treatment. Theranostics 11, 8813–8835.

Issa, N., Martin, C., Dulau, C., Camou, F., 2020. Severe anti-GFAP meningo-encephalomyelitis following viral infection. Mult. Scler. Relat. Disord. 45, 102448.

Jacob, F., Pather, S.R., Huang, W.-K., Zhang, F., Wong, S.Z.H., Zhou, H., Cubitt, B., Fan, W., Chen, C.Z., Xu, M., Pradhan, M., Zhang, D.Y., Zheng, W., Bang, A.G., Song, H., Carlos de la Torre, J., Ming, G.-l., 2020. Human pluripotent stem cell-derived neural cells and brain organoids reveal SARS-CoV-2 neurotropism predominates in choroid plexus epithelium. Cell Stem Cell 27 (6), 937–950.e9.

Jamieson, D.J., Rasmussen, S.A., 2022. An update on COVID-19 and pregnancy. Am. J. Obstet. Gynecol. 226, 177–186.

Joyce, Jonathan D., Greyson A. Moore, Poorna Goswami, Emma H. Leslie, Christopher K. Thompson, and Andrea S. Bertke. 2022. 'SARS-CoV-2 Infects Peripheral and Central Neurons of Mice Before Viremia, Facilitated by Neuropilin-1', *bioRxiv*: 2022.05.20.492834.

Krämer, B., Knoll, R., Bonaguro, L., ToVinh, M., Raabe, J., Astaburuaga-García, R., Schulte-Schrepping, J., Kaiser, K.M., Rieke, G.J., Bischoff, J., Monin, M.B., Hoffmeister, C., Schlabe, S., De Domenico, E., Reusch, N., Händler, K., Reynolds, G., Blüthgen, N., Hack, G., Finnemann, C., Nischalke, H.D., Strassburg, C.P., Stephenson, E., Su, Y., Gardner, L., Yuan, D., Chen, D., Goldman, J., Rosenstiel, P., Schmidt, S.V., Latz, E., Hrusovsky, K., Ball, A.J., Johnson, J.M., Koenig, P.A., Schmidt, F.I., Haniffa, M., Heath, J.R., Kümmerer, B.M., Keitel, V., Jensen, B., Stubbemann, P., Kurth, F., Sander, L.E., Sawitzki, B., Aschenbrenner, A.C., Schultze, J.L., Nattermann, J., 2021. Early IFN-α signatures and persistent dysfunction are distinguishing features of NK cells in severe COVID-19. Immunity 54, 2650-69.e14.

Li, J., Xu, Y., Ren, H., Zhu, Y., Peng, B., Cui, L., 2018. Autoimmune GFAP astrocytopathy after viral encephalitis: a case report. Mult. Scler. Relat. Disord. 21, 84–87.

Liu, H.Y., Guo, J., Zeng, C., Cao, Y., Ran, R., Wu, T., Yang, G., Zhao, D., Yang, P., Yu, X., Zhang, W., Liu, S.M., Zhang, Y., 2021. Transient early fine motor abnormalities in infants born to COVID-19 mothers are associated with placental hypoxia and ischemia. Front. Pediatr. 9, 793561.

Lodge, D.J., Grace, A.A., 2007. Aberrant hippocampal activity underlies the dopamine dysregulation in an animal model of schizophrenia. J. Neurosci. 27, 11424–11430.

Magri, A., Barbaglia, M.N., Foglia, C.Z., Boccato, E., Burlone, M.E., Cole, S., Giarda, P., Grossini, E., Patel, A.H., Minisini, R., Pirisi, M., 2017. 17, β-estradiol inhibits hepatitis C virus mainly by interference with the release phase of its life cycle. Liver Int. 37, 669–677.

Mao, L., Jin, H., Wang, M., Hu, Y., Chen, S., He, Q., Chang, J., Hong, C., Zhou, Y., Wang, D., Miao, X., Li, Y., Hu, B., 2020. 'Neurologic manifestations of hospitalized patients with coronavirus disease 2019 in Wuhan. China', *JAMA Neurol* 77, 1–9.

Martin, M., Paes, V.R., Cardoso, E.F., Cebp Neto, C.T., Kanamura, C.D.C., Leite, M.C.G., Otaduy, R.A.A., Monteiro, T., da Mauad, L.F.F., Silva, L.H.M., Castro, P.H.N., Saldiva, M.D., Duarte-Neto, A.N., 2022. Postmortem brain 7T MRI with minimally invasive pathological correlation in deceased COVID-19 subjects. Insights Imaging 13, 7.

Mateus, D., Sebastião, A.I., Carrascal, M.A., Carmo, A.D., Matos, A.M., Cruz, M.T., 2022. Crosstalk between estrogen, dendritic cells, and SARS-CoV-2 infection. Rev. Med. Virol. 32, e2290.

McCracken, I.R., Saginc, G., He, L., Huseynov, A., Daniels, A., Fletcher, S., Peghaire, C., Kalna, V., Andaloussi-Mäe, M., Muhl, L., Craig, N.M., Griffiths, S.J., Haas, J.G., Tait-Burkard, C., Lendahl, U., Birdsey, G.M., Betsholtz, C., Noseda, M., Baker, A.H., Randi, A.M., 2021. Lack of evidence of angiotensin-converting enzyme 2 expression and replicative infection by SARS-CoV-2 in human endothelial cells. Circulation 143 (8), 865–868.

McMahon, C.L., Staples, H., Gazi, M., Carrion, R., Hsieh, J., 2021. SARS-CoV-2 targets glial cells in human cortical organoids. Stem Cell Rep. 16, 1156–1164.

Meertens, L., Labeau, A., Dejarnac, O., Cipriani, S., Sinigaglia, L., Bonnet-Madin, L., Le Charpentier, T., Hafirassou, M.L., Zamborlini, A., Cao-Lormeau, V.M., Coulpier, M., Missé, D., Jouvenet, N., Tabibiazar, R., Gressens, P., Schwartz, O., Amara, A., 2017. Axl mediates ZIKA virus entry in human glial cells and modulates innate immune responses. Cell Rep. 18, 324–333.

Mesci, Pinar, Angela Macia, Aurian Saleh, Laura Martin-Sancho, Xin Yin, Cedric Snethlage, Simoni Avansini, Sumit K. Chanda, and Alysson Muotri. 2020. 'Sofosbuvir protects human brain organoids against SARS-CoV-2', *bioRxiv*: 2020.05.30.125856.

Mihaljevic, S., Michalicova, A., Bhide, M., Kovac, A., 2021. Pathophysiology of the choroid plexus in brain diseases. Gen. Physiol. Biophys. 40, 443–462.

Moghimi, N., Di Napoli, M., Biller, J., Siegler, J.E., Shekhar, R., McCullough, L.D., Harkins, M.S., Hong, E., Alaouieh, D.A., Mansueto, G., Divani, A.A., 2021. The neurological manifestations of post-acute sequelae of SARS-CoV-2 infection. Curr. Neurol. Neurosci. Rep. 21, 44.

Moreau, G.B., Burgess, S.L., Sturek, J.M., Donlan, A.N., Petri, W.A., Mann, B.J., 2020. Evaluation of K18-hACE2 mice as a model of SARS-CoV-2 infection. Am. J. Trop. Med. Hyg. 103, 1215–2129.

Moseby-Knappe, M., Mattsson-Carlgren, N., Stammet, P., Backman, S., Blennow, K., Dankiewicz, J., Friberg, H., Hassager, C., Horn, J., Kjaergaard, J., Lilja, G., Rylander, C., Ullén, S., Undén, J., Westhall, E., Wise, M.P., Zetterberg, H., Nielsen, N., Cronberg, T., 2021. Serum markers of brain injury can predict good neurological outcome after out-of-hospital cardiac arrest. Intensive Care Med. 47, 984–994.

Muldoon, K.M., Fowler, K.B., Pesch, M.H., Schleiss, M.R., 2020. SARS-CoV-2: Is it the newest spark in the TORCH? J. Clin. Virol. 127, 104372.

Muzio, L., Viotti, A., Martino, G., 2021. Microglia in neuroinflammation and neurodegeneration: from understanding to therapy. Front. Neurosci. 15, 742065.

Nagy Jr., B., Fejes, Z., Szentkereszty, Z., Sütő, R., Várkonyi, I., Ajzner, É., Kappelmayer, J., Papp, Z., Tóth, A., Fagyas, M., 2021. A dramatic rise in serum ACE2 activity in a critically ill COVID-19 patient. Int. J. Infect. Dis. 103, 412–444.

Østergaard, L., 2021. SARS CoV-2 related microvascular damage and symptoms during and after COVID-19: Consequences of capillary transit-time changes, tissue hypoxia and inflammation. Physiol. Rep. 9, e14726.

Patel, S.K., Juno, J.A., Lee, W.S., Wragg, K.M., Hogarth, P.M., Kent, S.J., Burrell, L.M., 2021. Plasma ACE2 activity is persistently elevated following SARS-CoV-2 infection: implications for COVID-19 pathogenesis and consequences. Eur. Respir. J. 57 (5), 2003730.

Pellegrini, L., Albecka, A., Mallery, D.L., Kellner, M.J., Paul, D., Carter, A.P., James, L.C., Lancaster, M.A., 2020. SARS-CoV-2 infects the brain choroid plexus and disrupts the blood-CSF barrier in human brain organoids. Cell Stem Cell 27, 951-61.e5.

Piekos, S.N., Roper, R.T., Hwang, Y.M., Sorensen, T., Price, N.D., Hood, L., Hadlock, J.J., 2022. The effect of maternal SARS-CoV-2 infection timing on birth outcomes: a retrospective multicentre cohort study. The Lancet Digital Health 4, e95–e104.

Pillai, P., Joseph, J.P., Fadzillah, N.H.M., Mahmod, M., 2021. COVID-19 and Major organ thromboembolism: manifestations in neurovascular and cardiovascular systems. J. Stroke Cerebrovasc. Dis. 30, 105427.
Poyiadji, N., Shahin, G., Noujaim, D., Stone, M., Patel, S., Griffith, B., 2020. COVID-19-associated acute hemorrhagic necrotizing encephalopathy: imaging features. Radiology 296 (2), E119–E120.
Rasmussen, S.A., Jamieson, D.J., 2022. COVID-19 and Pregnancy. Infect. Dis. Clin. North Am. 36, 423–433.
Rathnasinghe, R., S. Strohmeier, F. Amanat, V. L. Gillespie, F. Krammer, A. García-Sastre, L. Coughlan, M. Schotsaert, and M. Uccellini. 2020. 'Comparison of Transgenic and Adenovirus hACE2 Mouse Models for SARS-CoV-2 Infection', *bioRxiv*.
Reagan-Steiner, S., Bhatnagar, J., Martines, R.B., Milligan, N.S., Gisondo, C., Williams, F. B., Lee, E., Estetter, L., Bullock, H., Goldsmith, C.S., Fair, P., Hand, J., Richardson, G., Woodworth, K.R., Oduyebo, T., Galang, R.R., Phillips, R., Belyaeva, E., Yin, X.M., Meaney-Delman, D., Uyeki, T.M., Roberts, D.J., Zaki, S.R., 2022. Detection of SARS-CoV-2 in neonatal autopsy tissues and placenta. Emerg. Infect. Dis. 28, 510–557.
Rhodes, M.C., Seidler, F.J., Abdel-Rahman, A., Tate, C.A., Nyska, A., Rincavage, H.L., Slotkin, T.A., 2004. Terbutaline is a developmental neurotoxicant: effects on neuroproteins and morphology in cerebellum, hippocampus, and somatosensory cortex. J. Pharmacol. Exp. Ther. 308, 529–537.
Richards, J.L., Hansen, C., Bredfeldt, C., Bednarczyk, R.A., Steinhoff, M.C., Adjaye-Gbewonyo, D., Ault, K., Gallagher, M., Orenstein, W., Davis, R.L., Omer, S.B., 2013. Neonatal outcomes after antenatal influenza immunization during the 2009 H1N1 influenza pandemic: impact on preterm birth, birth weight, and small for gestational age birth. Clin. Infect. Dis. 56 (9), 1216–1222.
Ronovsky, M., Berger, S., Zambon, A., Reisinger, S.N., Horvath, O., Pollak, A., Lindtner, C., Berger, A., Pollak, D.D., 2017. Maternal immune activation transgenerationally modulates maternal care and offspring depression-like behavior. Brain Behav. Immun. 63, 127–136.
Sacco, K., Castagnoli, R., Vakkilainen, S., Liu, C., Delmonte, O.M., Oguz, C., Kaplan, I.M., Alehashemi, S., Burbelo, P.D., Bhuyan, F., de Jesus, A.A., Dobbs, K., Rosen, L.B., Cheng, A., Shaw, E., Vakkilainen, M.S., Pala, F., Lack, J., Zhang, Y., Fink, D.L., Oikonomou, V., Snow, A.L., Dalgard, C.L., Chen, J., Sellers, B.A., Montealegre Sanchez, G.A., Barron, K., Rey-Jurado, E., Vial, C., Poli, M.C., Licari, A., Montagna, D., Marseglia, G.L., Licciardi, F., Ramenghi, U., Discepolo, V., Lo Vecchio, A., Guarino, A., Eisenstein, E.M., Imberti, L., Sottini, A., Biondi, A., Mató, S., Gerstbacher, D., Truong, M., Stack, M.A., Magliocco, M., Bosticardo, M., Kawai, T., Danielson, J.J., Hulett, T., Askenazi, M., Hu, S., Cohen, J.I., Su, H.C., Kuhns, D.B., Lionakis, M.S., Snyder, T.M., Holland, S.M., Goldbach-Mansky, R., Tsang, J.S., Notarangelo, L.D., 2022. Immunopathological signatures in multisystem inflammatory syndrome in children and pediatric COVID-19. Nat. Med. 28, 1050–1062.
Sahin, B.E., Celikbilek, A., Kocak, Y., Saltoglu, G.T., Konar, N.M., Hizmali, L., 2022. Plasma biomarkers of brain injury in COVID-19 patients with neurological symptoms. J. Neurol. Sci. 439, 120324.
Shapiro-Mendoza, C.K., Rice, M.E., Galang, R.R., Fulton, A.C., VanMaldeghem, K., Prado, M.V., Ellis, E., Anesi, M.S., Simeone, R.M., Petersen, E.E., Ellington, S.R., Jones, A.M., Williams, T., Reagan-Steiner, S., Perez-Padilla, J., Deseda, C.C., Beron, A., Tufa, A.J., Rosinger, A., Roth, N.M., Green, C., Martin, S., Lopez, C.D., deWilde, L., Goodwin, M., Pagano, H.P., Mai, C.T., Gould, C., Zaki, S., Ferrer, L.N., Davis, M.S., Lathrop, E., Polen, K., Cragan, J.D., Reynolds, M., Newsome, K.B., Huertas, M.M., Bhatangar, J., Quiñones, A.M., Nahabedian, J.F., Adams, L., Sharp, T. M., Hancock, W.T., Rasmussen, S.A., Moore, C.A., Jamieson, D.J., Munoz-Jordan, J. L., Garstang, H., Kambui, A., Masao, C., Honein, M.A., Meaney-Delman, D., 2017. Pregnancy Outcomes After Maternal Zika Virus Infection During Pregnancy - U.S. Territories, January 1, 2016-April 25, 2017. MMWR Morb. Mortal. Wkly Rep. 66, 615–621.
Shi, L., Fatemi, S.H., Sidwell, R.W., Patterson, P.H., 2003. Maternal influenza infection causes marked behavioral and pharmacological changes in the offspring. J. Neurosci. 23, 297–302.
Simon, E., Gouyon, J.B., Cottenet, J., Bechraoui-Quantin, S., Rozenberg, P., Mariet, A.S., Quantin, C., 2022. Impact of SARS-CoV-2 infection on risk of prematurity, birthweight and obstetric complications: a multivariate analysis from a nationwide, population-based retrospective cohort study. BJOG 129, 1084–1094.
Song, E., Zhang, C., Israelow, B., Lu-Culligan, A., Prado, A.V., Skriabine, S., Lu, P., Weizman, O.E., Liu, F., Dai, Y., Szigeti-Buck, K., Yasumoto, Y., Wang, G., Castaldi, C., Heltke, J., Ng, E., Wheeler, J., Alfajaro, M.M., Levavasseur, E., Fontes, B., Ravindra, N.G., Van Dijk, D., Mane, S., Gunel, M., Ring, A., Kazmi, S.A.J., Zhang, K., Wilen, C.B., Horvath, T.L., Plu, I., Haik, S., Thomas, J.L., Louvi, A., Farhadian, S.F., Huttner, A., Seilhean, D., Renier, N., Bilguvar, K., Iwasaki, A., 2021. Neuroinvasion of SARS-CoV-2 in human and mouse brain. J. Exp. Med. 218.
Stárka, L., Dušková, M., 2021. Androgens in SARS-CoV-2 coronavirus infections. Physiol. Res. 70, S145–S151.
Stefanou, M.I., Palaiodimou, L., Bakola, E., Smyrnis, N., Papadopoulou, M., Paraskevas, G.P., Rizos, E., Boutati, E., Grigoriadis, N., Krogias, C., Giannopoulos, S., Tsiodras, S., Gaga, M., Tsivgoulis, G., 2022. Neurological manifestations of long-COVID syndrome: a narrative review. Ther Adv Chronic Dis 13, 20406223221076890.
Sun, X., Liu, Y., Huang, Z., Xu, W., Hu, W., Yi, L., Liu, Z., Chan, H., Zeng, J., Liu, X., Chen, H., Yu, J., Chan, F.K.L., Ng, S.C., Wong, S.H., Wang, M.H., Gin, T., Joynt, G.M., Hui, D.S.C., Zou, X., Shu, Y., Cheng, C.H.K., Fang, S., Luo, H., Lu, J., Chan, M.T.V., Zhang, L., Wu, W.K.K., 2022. SARS-CoV-2 non-structural protein 6 triggers NLRP3-dependent pyroptosis by targeting ATP6AP1. Cell Death Differ. 29, 1240–1254.
Taherifard, E., Taherifard, E., 2020. Neurological complications of COVID-19: a systematic review. Neurol. Res. 42 (11), 905–912.
Tarr, A.J., Chen, Q., Wang, Y., Sheridan, J.F., Quan, N., 2012. Neural and behavioral responses to low-grade inflammation. Behav. Brain Res. 235, 334–341.
Tomonaga, K., 2004. Virus-induced neurobehavioral disorders: mechanisms and implications. Trends Mol. Med. 10, 71–77.
Tremblay, M.E., Madore, C., Bordeleau, M., Tian, L., Verkhratsky, A., 2020. Neuropathobiology of COVID-19: the role for glia. Front. Cell. Neurosci. 14, 592214.
Van Campen, H., Bishop, J.V., Abrahams, V.M., Bielefeldt-Ohmann, H., Mathiason, C.K., Bouma, G.J., Winger, Q.A., Mayo, C.E., Bowen, R.A., Hansen, T.R., 2020. Maternal influenza A virus infection restricts fetal and placental growth and adversely affects the fetal thymic transcriptome. Viruses 12.
Vandenbark, A.A., Offner, H., Matejuk, S., Matejuk, A., 2021. Microglia and astrocyte involvement in neurodegeneration and brain cancer. J. Neuroinflammation 18, 298.
Varga, Z., Flammer, A.J., Steiger, P., Haberecker, M., Andermatt, R., Zinkernagel, A.S., Mehra, M.R., Schuepbach, R.A., Ruschitzka, F., Moch, H., 2020. Endothelial cell infection and endotheliitis in COVID-19. Lancet 395, 1417–2148.
Varma, P., Lybrand, Z.R., Antopia, M.C., Hsieh, J., 2020. Novel targets of SARS-CoV-2 spike protein in human fetal brain development suggest early pregnancy vulnerability. Front. Neurosci. 14, 614680.
Wambier, C.G., Goren, A., 2020. Severe acute respiratory syndrome coronavirus 2 (SARS-CoV-2) infection is likely to be androgen mediated. J. Am. Acad. Dermatol. 83, 308–339.
Wang, M., Chang, W., Zhang, L., Zhang, Y., 2022. Pyroptotic cell death in SARS-CoV-2 infection: revealing its roles during the immunopathogenesis of COVID-19. Int. J. Biol. Sci. 18 (15), 5827–5848.
Wang, L., Qin, X., Liang, J., Ge, P., 2021. Induction of pyroptosis: a promising strategy for cancer treatment. Front. Oncol. 11, 635774.
Wei, S.Q., Bilodeau-Bertrand, M., Liu, S., Auger, N., 2021. The impact of COVID-19 on pregnancy outcomes: a systematic review and meta-analysis. CMAJ 193 (16), E540–E548.
Winkler, E.S., Chen, R.E., Alam, F., Yildiz, S., Case, J.B., Uccellini, M.B., Holtzman, M.J., Garcia-Sastre, A., Schotsaert, M., Diamond, M.S., 2022. SARS-CoV-2 Causes lung infection without severe disease in human ACE2 knock-In mice. J. Virol. 96, e0151121.
Wölfel, R., Corman, V.M., Guggemos, W., Seilmaier, M., Zange, S., Müller, M.A., Niemeyer, D., Jones, T.C., Vollmar, P., Rothe, C., Hoelscher, M., Bleicker, T., Brünink, S., Schneider, J., Ehmann, R., Zwirglmaier, K., Drosten, C., Wendtner, C., 2020. Virological assessment of hospitalized patients with COVID-2019. Nature 581, 465–549.
Xu, P., Shan, C., Dunn, T.J., Xie, X., Xia, H., Gao, J., Allende Labastida, J., Zou, J., Villarreal, P.P., Schlagal, C.R., Yu, Y., Vargas, G., Rossi, S.L., Vasilakis, N., Shi, P.Y., Weaver, S.C., Wu, P., 2020. Role of microglia in the dissemination of Zika virus from mother to fetal brain. PLoS Negl. Trop. Dis. 14, e0008413.
Ye, C., Chiem, K., Park, J.G., Silvas, J.A., Morales Vasquez, D., Sourimant, J., Lin, M.J., Greninger, A.L., Plemper, R.K., Torrelles, J.B., Kobie, J.J., Walter, M.R., de la Torre, J.C., Martinez-Sobrido, L., 2021. Analysis of SARS-CoV-2 infection dynamic in vivo using reporter-expressing viruses. PNAS 118.
Yu, P., Zhang, X., Liu, N., Tang, L., Peng, C., Chen, X., 2021. Pyroptosis: mechanisms and diseases. Signal Transduct. Target. Ther. 6, 128.
Yue, J.K., Upadhyayula, P.S., Avalos, L.N., Deng, H., Wang, K.K.W., 2020. The Role of Blood Biomarkers for Magnetic Resonance Imaging Diagnosis of Traumatic Brain Injury. Medicina (Kaunas) 56.
Zambrano, L.D., Ellington, S., Strid, P., Galang, R.R., Oduyebo, T., Tong, V.T., Woodworth, K.R., Nahabedian, J.F., Azziz-Baumgartner, E., Gilboa, S.M., Meaney-Delman, D., Akosa, A., Bennett, C., Burkel, V., Chang, D., Delaney, A., Fox, C., Griffin, I., Hsia, J., Krause, K., Lewis, E., Manning, S., Mohamoud, Y., Newton, S., Neelam, V., Olsen, E.O., Perez, M., Reynolds, M., Riser, A., Rivera, M., Roth, N.M., Sancken, C., Shinde, N., Smoots, A., Snead, M., Wallace, B., Whitehill, F., Whitehouse, E., Zapata, L., 2020. Update: characteristics of symptomatic women of reproductive age with laboratory-confirmed SARS-CoV-2 infection by pregnancy status - united states, January 22-October 3, 2020. MMWR Morb. Mortal. Wkly Rep. 69 (44), 1641–1647.
Zhang, B.-Z., Chu, H., Han, S., Shuai, H., Deng, J., Hu, Y.-F., Gong, H.-R., Lee, A.-Y., Zou, Z., Yau, T., Wu, W., Hung, I.-N., Chan, J.-W., Yuen, K.-Y., Huang, J.-D., 2020. SARS-CoV-2 infects human neural progenitor cells and brain organoids. Cell Res. 30 (10), 928–931.
Zhang, Fengwen, Jesse Jenkins, Renan V. H. de Carvalho, Sandra Nakandakari-Higa, Teresia Chen, Morgan Abernathy, Elisabeth Nyakatura, David Andrew, Irina Lebedeva, Ivo Lorenz, H. Heinrich Hoffmann, Charles Rice, Gabriel Victora, Christopher Barnes, Theodora Hatziioannou, and Paul Bieniasz. 2022. "Human anti-ACE2 monoclonal antibodies as pan-sarbecovirus prophylactic agents." In.: bioRxiv.
Zhao, M., Jiang, X.F., Zhang, H.Q., Sun, J.H., Pei, H., Ma, L.N., Cao, Y., Li, H., 2021. Interactions between glial cells and the blood-brain barrier and their role in Alzheimer's disease. Ageing Res. Rev. 72, 101483.
Zhou, B., Thao, T.T.N., Hoffmann, D., Taddeo, A., Ebert, N., Labroussaa, F., Pohlmann, A., King, J., Steiner, S., Kelly, J.N., Portmann, J., Halwe, N.J., Ulrich, L., Trüeb, B.S., Fan, X., Hoffmann, B., Wang, L., Thomann, L., Lin, X., Stalder, H., Pozzi, B., de Brot, S., Jiang, N., Cui, D., Hossain, J., Wilson, M.M., Keller, M.W., Stark, T.J., Barnes, J.R., Dijkman, R., Jores, J., Benarafa, C., Wentworth, D.E., Thiel, V., Beer, M., 2021. SARS-CoV-2 spike D614G change enhances replication and transmission. Nature 592, 122–217.